

Original Article

The GroEL protein of *Porphyromonas gingivalis* regulates atherogenic phenomena in endothelial cells mediated by upregulating toll-like receptor 4 expression

Chun-Yao Huang^{1,2*}, Chun-Ming Shih^{1,2,3*}, Nai-Wen Tsao⁴, Yi-Wen Lin^{1,5}, Chun-Che Shih⁶, Kuang-Hsing Chiang^{1,2}, Song-Kun Shyue⁷, Yu-Jia Chang³, Chi-Kun Hsieh¹, Feng-Yen Lin^{1,2,3}

¹Department of Internal Medicine, School of Medicine, College of Medicine, Taipei Medical University, Taipei, Taiwan; ²Division of Cardiology and Cardiovascular Research Center, Department of Internal Medicine, Taipei Medical University Hospital, Taipei, Taiwan; ³Graduate Institute of Clinical Medicine, College of Medicine, Taipei Medical University, Taipei, Taiwan; ⁴Division of Cardiovascular Surgery, Taipei Medical University Hospital, Taipei; ⁵Institute of Oral Biology, National Yang-Ming University, Taipei, Taiwan; ⁶Division of Cardiovascular Surgery, Taipei Veterans General Hospital, Taipei, Taiwan; ⁷Institute of Biomedical Sciences, Academia Sinica, Taipei, Taiwan.
*Equal contributors.

Received September 5, 2015; Accepted January 2, 2016; Epub February 15, 2016; Published February 29, 2016

Abstract: *Porphyromonas gingivalis* (*P. gingivalis*) is a bacterial species that causes periodontitis. GroEL from *P. gingivalis* may possess biological activity and may be involved in the destruction of periodontal tissues. However, it is unclear whether *P. gingivalis* GroEL enhances the appearance of atherogenic phenomena in endothelial cells and vessels. Here, we constructed recombinant GroEL from *P. gingivalis* to investigate its effects in human coronary artery endothelial cells (HCAECs) *in vitro* and on aortas of high-cholesterol (HC)-fed B57BL/6 and B57BL/6-*Tlr4*^{lps-del} mice *in vivo*. The results showed that GroEL impaired tube-formation capacity under non-cytotoxic conditions in HCAECs. GroEL increased THP-1 cell/HCAEC adhesion by increasing the expression of intracellular adhesion molecule (ICAM)-1 and vascular adhesion molecule (VCAM)-1 in endothelial cells. Additionally, GroEL increased DiI-oxidized low density lipoprotein (oxLDL) uptake, which may be mediated by elevated lectin-like oxLDL receptor (LOX)-1 but not scavenger receptor expressed by endothelial cells (SREC) and scavenger receptor class B1 (SR-B1) expression. Furthermore, GroEL interacts with toll-like receptor 4 (TLR4) and plays a causal role in atherogenesis in HCAECs. Human antigen R (HuR), an RNA-binding protein with a high affinity for the 3' untranslated region (3'UTR) of TLR4 mRNA, contributes to the up-regulation of TLR4 induced by GroEL in HCAECs. In a GroEL animal administration study, GroEL elevated ICAM-1, VCAM-1, LOX-1 and TLR4 expression in the aortas of HC diet-fed wild C57BL/6 but not C57BL/6-*Tlr4*^{lps-del} mice. Taken together, our findings suggest that *P. gingivalis* GroEL may contribute to cardiovascular disorders by affecting TLR4 expression.

Keywords: *Porphyromonas gingivalis*, GroEL, atherosclerosis

Introduction

Periodontopathogenic bacteria may help to destroy periodontal tissues, including the gingiva, cementum, alveolar bone, and periodontal ligament, in periodontitis. However, their pathological effects are also due to their capacity to release a number of virulence factors, such as GroEL (belonging to the heat shock protein (HSP) 60 family) [1, 2], gingipains [3, 4], and lipopolysaccharide (LPS). There is evidence indicating that periodontopathogenic bacteria are associated with the occurrence of systemic complications such as cancer [5, 6], pulmonary

disease, atherosclerosis, preterm delivery, and diabetes in addition to periodontitis. Although nearly 700 bacterial species have been identified in the oral cavity, only some of them contribute to the initial incidence and continued persistence of periodontitis [7]. However, *Porphyromonas gingivalis* (*P. gingivalis*), a Gram-negative anaerobic bacterium that belongs to the phylum Bacteroidetes, is one of the common pathogens that induces periodontitis [8, 9]. More recently, *P. gingivalis*, which has a critical role in the progress of carcinoma [10], has the ability to prevent epithelial cell apoptosis and protect cancerous processes [11, 12] by

Porphyromonas gingivalis regulates atherogenesis

Table 1. Body weight, kidney and liver function (n=5) in experimental mice

	wk	Wild C57BL/6 mouse					C57BL/6- <i>Tlr4^{lps-del}</i> mouse		
		Normal diet		HC diet			Normal diet		HC diet
		-	-	GroEL 200 µg/kg BW	GroEL 400 µg/kg BW	GST 400 µg/kg BW	-	-	GroEL 400 µg/kg BW
BW (g)	0	24.2±1.0	23.4±0.7	24.2±0.5	22.7±0.4	24.3±2.2	22.6±1.5	22.5±3.1	25.0±1.4
	2	26.6±1.2	24.6±0.2	25.2±0.5	23.2±1.2	26.0±1.5	24.5±1.0	25.3±1.6	25.9±2.5
	4	26.0±0.5	25.1±1.1	27.9±1.1	26.3±1.3	26.4±1.2	25.8±0.9	26.4±2.1	27.4±3.7
BUN (mg/dL)	0	18.5±6.5	21.0±2.2	18.0±4.5	18.3±1.9	17.3±4.4	23.6±1.5	21.5±0.9	27.7±2.9
	2	23.5±3.5	22.3±5.8	18.8±3.5	16.5±1.1	18.3±3.0	22.9±1.0	21.9±2.4	24.0±4.2
	4	20.5±6.5	31.0±12.6	29.3±0.8	24.5±5.5	16.0±7.8	25.0±0.9	19.4±1.9	18.7±5.0
Cr (mg/dL)	0	0.4±0.2	0.8±0.4	0.6±0.2	0.5±0.2	0.6±0.2	0.3±0.1	0.5±0.1	0.8±0.1
	2	0.4±0.2	0.7±0.1	0.7±0.3	0.7±0.2	0.8±0.2	0.5±0.1	0.6±0.1	0.5±0.1
	4	0.8±0.2	0.6±0.2	0.7±0.2	0.6±0.4	0.6±0.2	0.6±0.2	0.7±0.3	0.6±0.2
ALT (IU/L)	0	129.2±4.6	114.5±11.6	113.5±12.2	118.9±9.2	119.9±6.9	124.7±6.2	128.3±5.7	115.0±7.1
	2	101.6±16.9	114.7±9.4	108.4±9.5	120.9±12.6	115.1±8.7	115.3±9.0	100.8±8.5	30.3±4.7
	4	127.5±4.3	118.1±9.8	119.0±4.4	112.8±15.4	126.8±2.7	104.7±5.4	98.4±9.9	30.7±3.8
AST (IU/L)	0	113.4±16.1	89.4±32.0	120.1±35.1	97.1±6.5	111.1±21.9	114.5±5.1	112.4±5.2	117.7±8.5
	2	129.0±2.6	113.4±37.5	115.4±13.6	114.3±20.4	114.7±14.8	108.7±7.8	104.4±4.1	127.1±8.8
	4	111.0±7.2	135.2±38.5	104.8±28.7	125.7±20.7	121.1±18.4	116.0±5.4	112.7±3.5	113.4±7.9
LDH (IU/L)	0	1968.2±863.6	2113.9±306.8	1802.3±452.8	1967.2±896.2	1627.9±73.3	1559.6±107.4	1942.3±196.7	2049.5±106.9
	2	1561.3±110.0	1903.6±321.7	2317.6±639.3	2239.4±219.2	2550.6±313.6	1848.6±289.7	1945.8±366.2	2148.6±520.3
	4	1373.2±248.7	1998.5±316.8	2594.3±249.8	2604.8±152.3	2263.9±652.9	1651.3±176.9	2356.3±508.7	2259.6±421.2

BW, Body weight; HC diet, High cholesterol diet; BUN, blood urea nitrogen; Cr, Creatinine; ALT, alanine aminotransferase; AST, aspartate aminotransferase; LDH, lactate dehydrogenase. Values are mean ± SD.

manipulating intercellular signaling pathways [13]. Moreover, it is well known that GroEL had been recognized as an important molecule in bacterial infectious diseases [14, 15]. GroEL stimulates the production of inflammatory cytokines such as interleukin (IL)-6 and IL-8 in human monocytes [16-18], gingival epithelial cells, and gingival fibroblasts [19-21] and also up-regulates the expression of adhesion molecules [22, 23]. Patients suffering from periodontitis show higher titers of anti-*P. gingivalis* GroEL antibody than do healthy subjects, indicating that GroEL induces an immune response in patients with periodontitis [1, 2]. A vaccine directed against the GroEL of *P. gingivalis* may reduce periodontitis-associated alveolar bone loss [24]. *P. gingivalis* GroEL can stimulate the activation of NF- κ B during inflammation, which may be reversed by the inhibition of toll-like receptor (TLR) 2 and TLR4 in THP-1 cells [25]. Therefore, GroEL from *P. gingivalis* is a critical immunodominant antigen that may contribute to pathogenic processes and inflammation.

Atherosclerosis is a systemic disease mediated by chronic inflammation, including the involvement of complex cell-molecular mechanisms and risk factors. In the clinic, periodontopathogenic bacteria are associated with atherosclerosis. Although GroEL from *P. gingivalis* was demonstrated to be a potent stimulator of cytokines in periodontitis and systemic inflammation, many critical confounding effects of GroEL related to atherogenesis are unclear. Therefore, in this study, we investigated the influence of GroEL from *P. gingivalis* on human coronary artery endothelial cells (HCAECs) and the aortas of mice. We constructed a recombinant GroEL from *P. gingivalis*. A cell migration assay, tube formation assay, HCAECs/THP-1 adhesion assay, actinomycin D chase experiment, western blot analysis, 1,1'-dioctadecyl-3,3,3',3'-tetramethyl-indocarbocyanine perchlorate (DiI)-labeled oxidized low density lipoprotein (oxLDL) uptake assay, luciferase reporter assay, and immunohistochemical staining were performed. *In vitro* results showed that GroEL impaired the capacity of tube formation and cell migration. GroEL increased the adhesiveness of THP-1 cells to HCAECs by increasing the expression of the adhesion molecules vascular adhesion molecule (VCAM)-1 and intracellular adhesion molecule (ICAM)-1. Additionally, GroEL increased DiI-labeled oxLDL uptake, which may be mediated by elevated lectin-like oxLDL

receptor (LOX)-1 but not scavenger receptors expressed by endothelial cells (SREC) and scavenger receptor class B1 (SR-B1) expression. Furthermore, GroEL interacts with TLR4 and plays a causal role in atherogenesis in HCAECs. Human antigen R (HuR), an RNA-binding protein with a high affinity for the 3' untranslated region (3'UTR) of TLR4 mRNA, contributes to the up-regulation of TLR4 induced by GroEL in HCAECs. In animal studies, the systemic inflammation induced by GroEL elevated ICAM-1, VCAM-1, LOX-1 and TLR4 expression in C57BL/6 but not C57BL/6-*Tlr4*^{lps-del} mice. Taken together, our findings suggest that GroEL protein of *P. gingivalis* may contribute to cardiovascular disorders.

Materials and methods

Construction of *P. gingivalis* GroEL expression vectors

The genomic DNA of *Porphyromonas (P.) gingivalis* (ATCC No. 33277) was extracted using the EasyPure Genomic DNA mini kit (Bioman Scientific Co., Taipei, Taiwan). The open reading frame of GroEL was originally PCR-amplified using 100 ng of *P. gingivalis* genomic DNA as a template, 0.2 mM dNTPs, 1 mM each of gene specific primers and 1 U Pfu DNA polymerase (Promega, WI, USA) with the following program: one cycle of 95°C for 5 min; 38 cycles of 95°C for 45 sec, 68°C for 45 sec, and 72°C for 2 min; and 1 cycle of 68°C for 45 sec and 72°C for 10 min with a final incubation at 72°C for 10 min with 1 U Taq DNA polymerase. The GroEL-specific forward and reverse primers used in the PCR reaction are shown in **Table 1**. The amplified GroEL cDNA fragment was then cloned into the *pCR2.1-TOPO* vector (Invitrogen, CA, USA) and subsequently cloned in-frame into the EcoRI sites of the pGEX-5X-1 expression vector (*GE Healthcare Amersham Biosciences*, CA, USA) for expression in *E. coli* (DH5a).

Purification of recombinant GroEL protein

BL21 cells were transformed with the pGEX-5X-1-GroEL expression vector, and the recombinant GroEL protein was purified. Briefly, BL21 cells (RBC Bioscience, New Taipei City, Taiwan) containing the plasmid pGEX-5X-1-GroEL were grown overnight at 37°C in 2 mL of LB medium supplemented with 100 μ g/mL ampicillin.

Porphyromonas gingivalis regulates atherogenesis

Then, 1.25 mL of overnight culture was transferred into 100 mL of LB/ampicillin medium and grown at 37°C to an A600 of 0.6-0.8 (approximately 2 h). Expression of the fusion protein was then induced by adding IPTG to a final concentration of 1 mM at 30°C for 6 h. The bacteria were pelleted by centrifugation for 10 min at 8000 rpm, and recombinant GroEL was extracted under native conditions using the GST Gene Fusion System according to the manufacturer's instructions (*GE Healthcare Amersham Biosciences*, CA, USA). Finally, the recombinant GroEL protein was purified with elution buffer containing 50 mM Tris-HCl and 10 mM reduced glutathione (pH 8.0). The quantity of recombinant GroEL protein was measured using the Bio-Rad Protein Assay (Bio-Rad, Hercules, CA, USA). The fusion protein was detected by SDS gel electrophoresis and identified by immunoblotting with a GST antibody (*GE Healthcare Amersham Biosciences*, CA, USA). The endotoxin levels in the recombinant GroEL protein preparation were measured using a Limulus Amebocyte Lysate kit from Cambrex Inc. in the USA. The LPS levels were below 1 pg/mL.

Cell culture

HCAECs were purchased from Cascade Biologics, Inc. (Portland, OR, USA). Human monocytic THP-1 cells were purchased from American Type Culture Collection (Manassas, VA, USA). Cell culturing and passages were performed according to the manufacturer's instructions.

Measurement of cytotoxicity by MTT assay

The cytotoxicity of GroEL was analyzed using the 3-(4,5-dimethylthiazol-2-yl)-2,5-diphenyltetrazolium bromide (MTT) assay. HCAECs (2×10^4 cells) were grown in 96-well plates and incubated with GroEL at 0.5-5 $\mu\text{g}/\text{mL}$ for 8-48 hours. Subsequently, MTT (0.5 $\mu\text{g}/\text{mL}$) was applied to the cells for 4 h to allow the conversion of MTT into formazan crystals. After washing with PBS, the cells were lysed with dimethyl sulfoxide, and the absorbance was read at 530 nm with a DIAS Microplate Reader (Dynex Technologies, VA, USA).

Wound-healing assay of HCAEC migration

The migratory function of HCAECs, which is essential for maintaining normal vascular function, was evaluated using a wound-healing

assay. HCAECs were cultured in a 12-well plate. The confluent cells (approximately 2×10^5 cells/well) were wounded by scraping with a 100- μL pipette tip, which denuded a strip of the monolayer that was 300 μm in diameter. The cells were supplied with medium containing 5% fetal bovine serum, and the rate of wound closure was observed after 24 h. The distance of the gap was measured under the 4x phase objective of a light microscope (OLYMPUS IX71, Tokyo, Japan), monitored with a CCD camera (Macro FIRE 2.3A), and captured with a video graphic system (Picture Frame Application 2.3 software).

HCAEC tube formation assay

Tube formation assays were performed on HCAECs to assess angiogenic capacity, which is believed to be important for endothelium function. The *in vitro* tube formation assays were performed using the Angiogenesis Assay Kit (Chemicon, CA, USA) [26] according to the manufacturer's protocol. Briefly, ECMatrix gel solution was thawed at 4°C overnight, mixed with ECMatrix diluent buffer, and placed in a 96-well plate at 37°C for 1 hour to allow the matrix solution to solidify. HCAECs were treated with GroEL for 24 hours and then harvested. A total of 10^4 cells were placed on the matrix solution, and the samples were incubated at 37°C for 8 hours. Tubule formation was inspected under an inverted light microscope, and four representative fields were taken. The average of the total area of complete tubes formed by cells was compared using the Image-Pro Plus computer software.

HCAEC/THP-1 cell adhesion assay

HCAECs (5×10^5) were distributed into 24-well plates before the assay. Then, the growth medium was supplemented with GroEL at the indicated concentrations for 24 h. THP-1 cells were labeled for 1 h at 37°C with 10 mM of 2,7-bis(2-carboxyethyl)-5(6)-carboxyfluorescein acetoxymethyl ester (BCECF/AM, Boehringer-Mannheim) in serum-free RPMI 1640 medium; they were then washed with PBS to remove free dye and resuspended in RPMI 1640 containing 2% FBS. One million labeled THP-1 cells were added to each HCAEC-containing well, and incubation continued for 1 h. Non-adherent cells were removed by three gentle washes with HBSS. The degree of THP-1 cells adhered to the

Porphyromonas gingivalis regulates atherogenesis

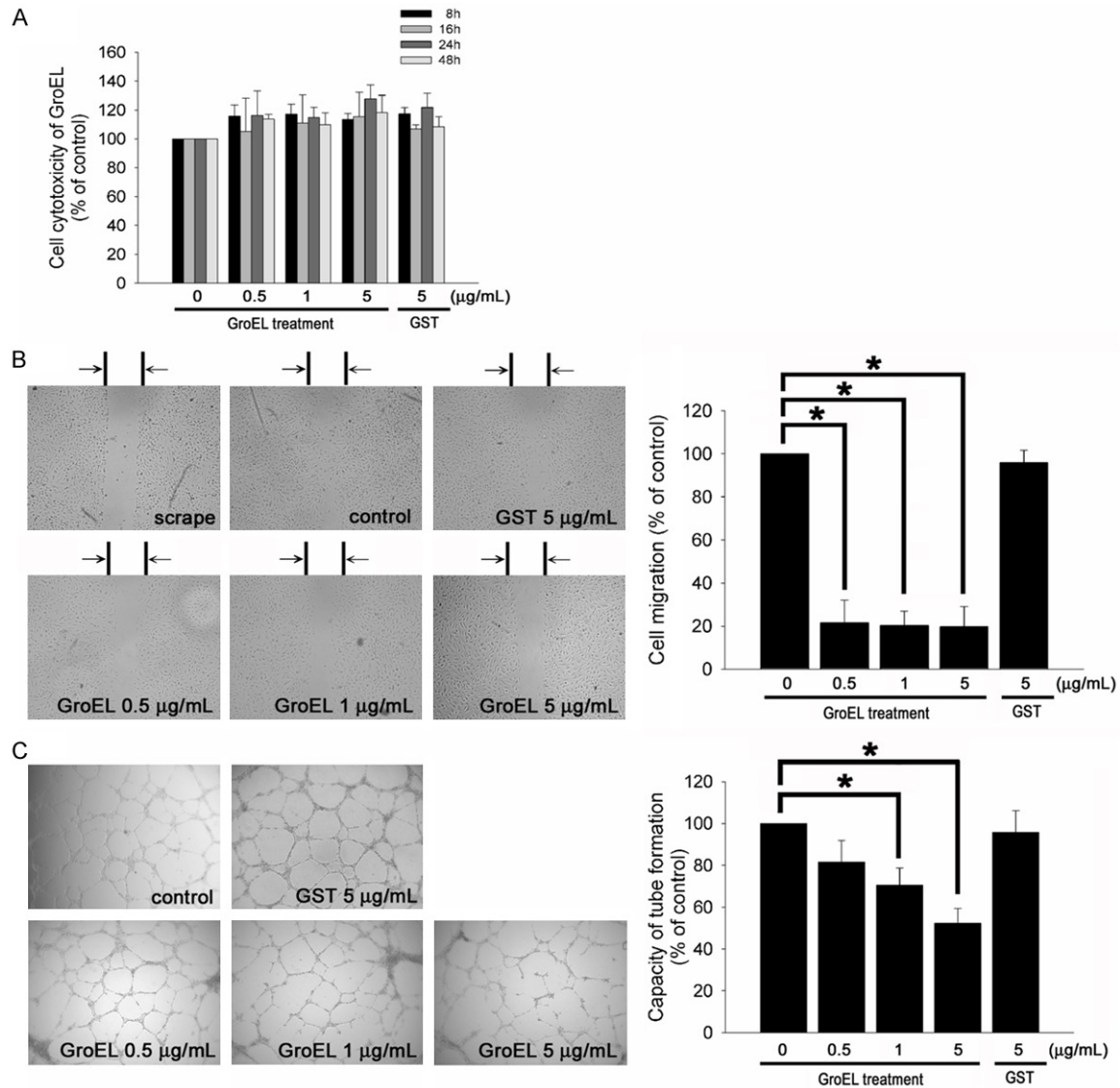


Figure 1. GroEL decreased the activity of HCAECs without impairing their viability. **A.** Treatment of HCAECs with 0.5-5 µg/mL of GroEL protein for 8-48 hours; cell cytotoxicity of GroEL was analyzed by MTT assay, and the absorbance was recorded using a microplate reader. All data are expressed as the mean ± SEM of three experiments performed in triplicate and as a percentage of the control. Statistical evaluation was performed using two-way ANOVA followed by a Dunnett's test. **B.** Wound-healing assay for evaluating the effect of GroEL on HCAEC migration. HCAECs migrating to the denuded area were counted based on the black baseline. EPCs were cultured with GroEL or GST for 24 hours before wound scraping using a pipette tip. The photographs were taken 10 hours after wound scraping. The HCAECs that migrated into the denuded area (double arrows were indicated the denuded area) were analyzed; the magnitude of HCAEC migration was evaluated by counting the migrated cells in six random clones under a high-power microscope field (x100). **C.** HCAECs were pretreated with GroEL or GST for 24 hours. An *in vitro* tube formation assay was performed using ECMatrix gel to investigate the effect of GroEL on the HCAECs' lining function. The photographs were taken 8 hours after seeding of HCAECs. All data are expressed as the mean ± SEM of three experiments performed in triplicate and as a percentage of the control. Statistical evaluation was performed using one-way ANOVA followed by a Dunnett's test. * $p < 0.05$ compared with control (without GroEL treatment).

HCAECs was observed using inverted fluorescent microscopy and counted using a Multilabel Counter Victor² (Wallace, CA, USA) at an emission of 530 nm and an absorption of 435 nm after the cells were lysed with DMSO.

Western blot analysis

Total cell lysate, nuclear, and membrane proteins were processed according to previous reports [27]. The protein concentration in the

supernatant was measured using a Bio-Rad protein determination kit (Bio-Rad, CA, USA). The supernatants were subjected to 8% SDS-PAGE and transferred for 1 hour at room temperature to polyvinylidene difluoride membranes. The membranes were treated for 1 hour at room temperature with PBS containing 0.05% Tween-20 and 2% skimmed milk and incubated separately for 1 hour at room temperature with primary antibodies. The membranes were then incubated with horseradish peroxidase-conjugated IgG. Immunodetection was performed using a chemiluminescence reagent and with exposure to VersaDoc Imaging System 5000MP (Bio-Rad, CA, USA).

Uptake of Dil-labeled oxLDL by HCAECs

Human LDL (d:1.019-1.063 g/ml) was isolated by sequential ultracentrifugation of fasting plasma samples from healthy adult males. The native LDL was oxidized and labeled with Dil as described previously [28, 29]. To examine cellular uptake of oxLDL, HCAECs were seeded on culture slides and incubated for 4 hours in culture medium containing 80 µg/mL of Dil-labeled oxLDL. At the end of the treatment, the cells were washed with PBS, mounted on cover slips, examined with confocal microscopy and counted using a Multilabel Counter Victor2 (Wallace, CA, USA) after the cells were lysed with DMSO.

Quantitative real time and traditional polymerase chain reaction

Total RNA was isolated using a TRIZOL reagent kit (Invitrogen, CA, USA). cDNA was synthesized from total RNA using Superscript® II reverse transcriptase. Quantitative real time polymerase chain reaction (PCR) was performed using a FastStart DNA Master SYBR Green I kit and LightCycler (Roche, CA, USA). FastStart Taq DNA polymerase was activated by incubation at 95°C for 2 min before 40 cycles of 95°C for 1 s, 60°C for 5 s, and 72°C for 7 s. Fluorescence was measured at 86°C after the 72°C extension step. The level of TLR4 mRNA expression were determined in arbitrary units by comparison with an external DNA standard that was amplified by the TLR4 primers. Traditional PCR was performed using Promega PCR reagents. Amplification of GAPDH was performed in the same samples to verify RNA abundance. The PCR mixture was amplified in a DNA thermal

cycler (Biometra T3, Berlin, Germany) with 30 cycles for GAPDH (denaturation at 95°C for 1 min, annealing at 53°C for 1 min and extension at 75°C for 2 min). The PCR primers used for amplification of TLR4 and GAPDH were: TLR4 forward primer: 5'-AAG CCG AAA GGT GAT TGT TG-3', reverse primer: 5'-CTG TCC TCC CAC TCC AGG TA-3'; GAPDH forward primer: 5'-TGC CCC CTC TGC TGA TGC C-3', reverse primer: 5'-CCT CCG ACG CCT GCT TCA CCA C-3'. All specific primers were synthesized by Sigma-Aldrich (MO, USA).

Actinomycin D chase experiment

Actinomycin D (20 µg/mL) was added to cells for 1 h following their treatment under various experimental conditions. Total RNA was extracted at 0, 30, 60, 120, 240, and 300 min after the addition of actinomycin D, and quantitative real time PCR was performed. The half-life ($t_{1/2}$) of the TLR4 mRNA was calculated according to the following formula $t_{1/2} = 0.693/k$, where $k = \ln(N_0/N_t)/t$ in which N_0 is the cross-point of real-time PCR at $t = 0$ and N_t is the cross-point at time t .

Construction of luciferase reporter plasmids containing the 3'UTR of TLR4 mRNA

According to a previous report [30], we had generated a CMV promoter-derived luciferase reporter plasmid for expression in mammalian cells. The following specific primers were used in the PCR reaction: TLR4-3'UTR Pr-forward: TGACC CACAA GTBAA AAAGG and TLR4-3'UTR Pr-reverse: TCCCA GCCAT CTGTG TCTC.

Luciferase reporter assay and transfection

Functional analysis of the 3'UTR of TLR4 mRNA was performed using plasmids containing the 3'UTR and a luciferase reporter gene (from pGL-Basic vector (Promega, USA)). A total of 10^6 cells were trypsinized and resuspended in 100 ml of Nucleofector solution; 1 mg of the reporter plasmid (CMV-Luciferase-TLR4 3'UTR sense, and CMV-Luciferase-TLR4 3'UTR antisense) was transfected using the Nucleofector electroporation device according to the manufacturer's instructions. Equal amounts of the luciferase reporter gene containing pcDNA3.1 plasmid (CMV-Luciferase) was used as a control group. Transfection efficiency was normalized to uniformity using a β -galactosidase reporter

Porphyromonas gingivalis regulates atherogenesis

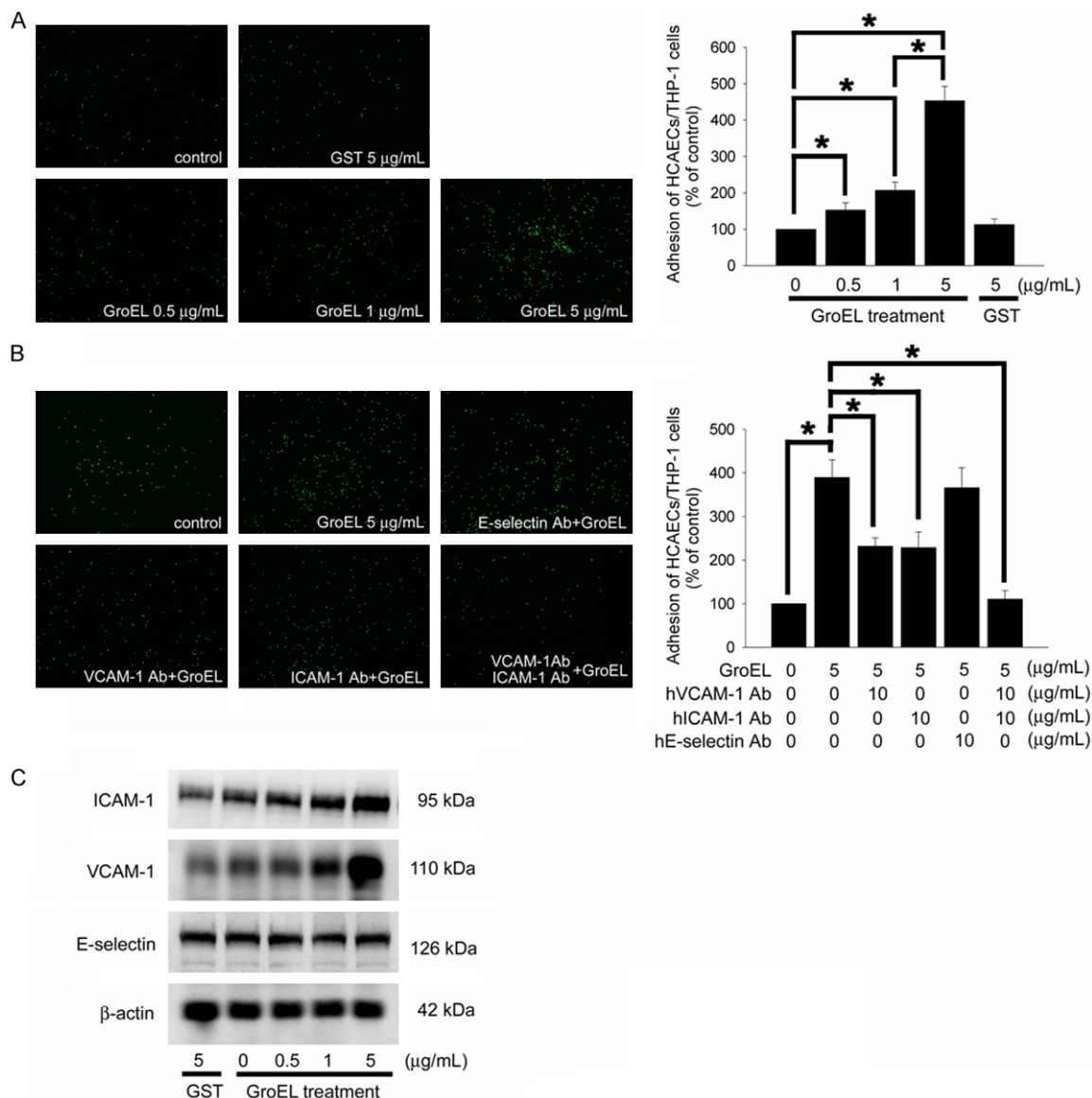
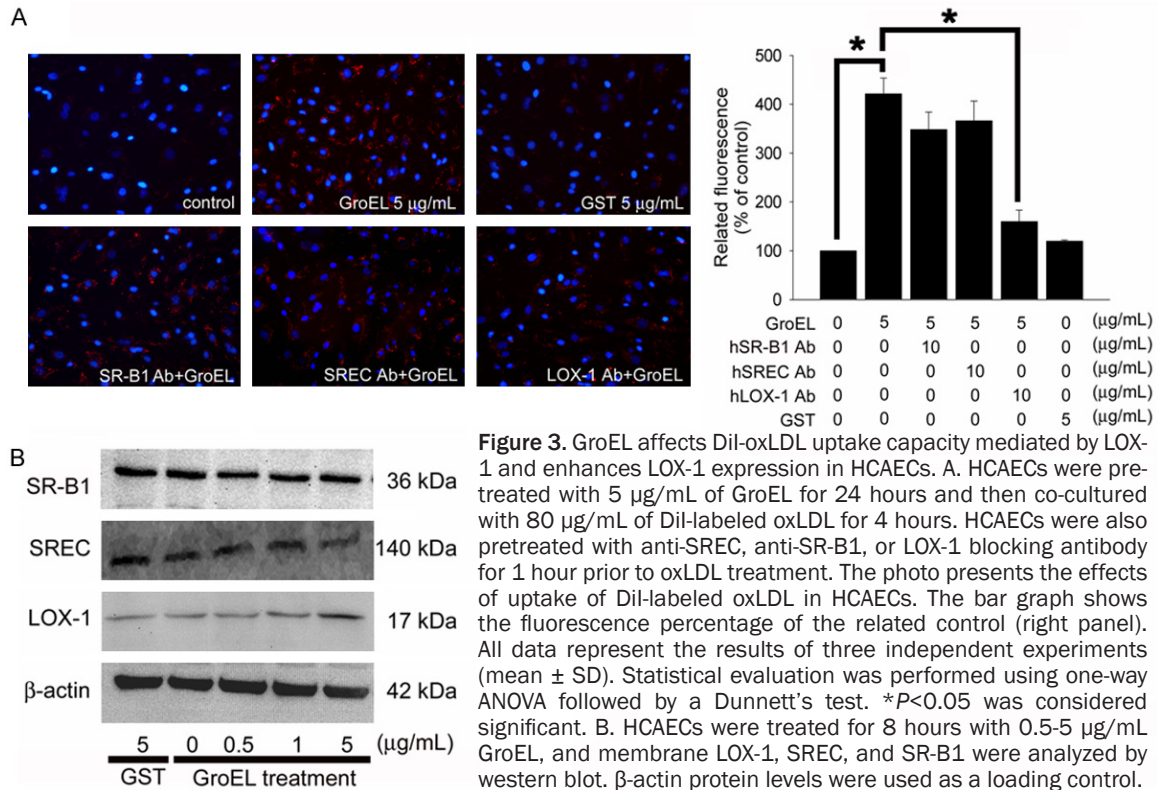


Figure 2. GroEL induces VCAM-1 and ICAM-1 expression, which mediates HCAEC/THP-1 cell adhesion. A. HCAECs were pretreated with 0.5-5 $\mu\text{g/mL}$ of GroEL for 24 hours and then co-cultured with THP-1 cells for 1 hour. B. Cells were pretreated with GroEL for 24 hours, followed by anti-hE-selectin, anti-hVCAM-1 or anti-hICAM-1 antibody treatment for 30 min. HCAECs and THP-1 cells were co-cultured for 1 hour. The degree of THP-1 adhesion to the HCAECs was counted using a Multilabel Counter Victor². Treatment with 5 $\mu\text{g/mL}$ GST served as a negative control. Isotype IgG was also used as a negative control. The bar graph demonstrates the adhesion percentage of the control. All data represent the results of three independent experiments (mean \pm SD). Statistical evaluation was performed using one-way ANOVA followed by a Dunnett's test. * $P < 0.05$ was considered significant. C. HCAECs were stimulated for 8 hours with 0.5-5 $\mu\text{g/mL}$ of GroEL. Treatment with GST served as a negative control. Western blot analyses of E-selectin, VCAM-1, and ICAM-1 proteins were performed. Total β -actin protein was used as a loading control.

plasmid. Cell extracts were prepared with reporter lysis buffer (300 μl /well), protein concentrations were determined, and the luciferase activity was quantified by luminometry (Wallac Victor², Finland) using the luciferase assay system (Promega, CA, USA). b-galactosidase activity was measured using a b-galactosidase enzyme assay kit (Stratagene, CA, USA).

Animal experiment

Forty male C57BL/6 mice were purchased from BioLASCO Taiwan Co., Ltd (Yi-Lan, Taiwan), and fifteen male C57BL/6-*Tlr4*^{lps-del} mice (a TLR4-knockout mouse homozygous for the defective LPS-response deletion allele *Tlr4*^{lps-del}) were purchased from the Jackson Laboratory (JAX®),



003752, ME, USA). All animals were treated according to protocols approved by the Institutional Animal Care Committee of the Taipei Medical University, Taipei, Taiwan (admission No.: LAC-100-0161). The experimental procedures and animal care conformed to the "Guide for the Care and Use of Laboratory Animals" published by the U.S. National Institutes of Health (NIH Publication No. 85-23, revised 1996). All mice were kept in microisolator cages on a 12-h day/night cycle and fed commercial normal mouse chow diet (Scientific Diet Services, Essex, UK) or DIO rodent purified high cholesterol (HC) diet (TestDiet, MO, USA) with water *ad libitum*. The animals were divided into eight groups (5 animals/per group). C57CL/B6 mice were included in groups 1-5 and C57BL/6-*Tlr4^{lps-del}* mice were included in groups 6-8. Group 1 (naïve control): C57CL/B6 mice fed with normal chow diet; group 2: C57CL/B6 mice fed with high cholesterol (HC) diet; group 3: C57CL/B6 mice fed with HC diet and receiving a tail vein injection of 200 µg/kg body weight (BW) of GroEL twice a week throughout the experiment (28 days); group 4: C57CL/B6 mice fed with HC diet and receiving a tail vein injection of 400 µg/kg BW of GroEL; group 5:

C57CL/B6 mice fed with HC diet and receiving a tail vein injection of 400 µg/kg BW of GST; group 6: C57BL/6-*Tlr4^{lps-del}* mice fed with normal chow diet; group 7: C57BL/6-*Tlr4^{lps-del}* mice fed with HC diet; group 8: C57BL/6-*Tlr4^{lps-/-}* mice fed with HC diet and receiving a tail vein injection of 400 µg/kgBW of GroEL. At the end of the experiment (day 28), the mice were sacrificed and the thoracic aorta were removed.

Biochemical measurements

Blood samples for biochemical measurements were collected from each animal before the start of the experiment and at the end of weeks 2 and 4. Samples were collected from the mandibular artery into sodium citrate-containing tubes under no sedation and were used and separated by centrifugation. Serum blood urea nitrogen (BUN), creatinine (Cr), alanine aminotransferase (ALT), aspartate aminotransferase (AST), lactate dehydrogenase (LDH), total-cholesterol, triglyceride (TG), high density lipoprotein (HDL), and low density lipoprotein (LDL), were measured using the SPOTCHEM™ SP-4410 automatic dry chemistry system (Arkray, Tokyo, Japan).

Immunohistochemistry

Histopathological features of 5- μ m-thick paraffin-embedded cross-sections of mouse aortas were stained using hematoxylin and eosin. Immunohistochemical staining used anti-oxLDL (Biossusa, MA, USA), anti-VCAM-1 (abcam, CA, USA), anti-ICAM-1 (Novusbio, CA, USA), anti-LOX-1 (Santa Cruz, CA, USA) anti-scavenger receptor expressed by endothelial cells (SREC; Santa Cruz, CA, USA), scavenger receptor B1 (SR-B1; Santa Cruz, CA, USA), anti-TLR4 (Santa Cruz, CA, USA), or anti-CD68 (GeneTex, CA, USA) antibodies. The slides were observed via microscopy.

Statistical analysis

Values are expressed as the mean \pm SEM. Statistical evaluation was performed using one- or two-way ANOVA followed by a Dunnett's test. A probability value of $p < 0.05$ was considered significant.

Results

In vitro study

GroEL decreased migration and tube formation even though it did not impair the viability of HCAECs: An MTT assay was performed to analyze cell viability and the cytotoxicity of GroEL. HCAECs were treated with 0.5-5 μ g/mL of GroEL for 8, 16, 24, or 48 hours. The results showed that treatment with GroEL at 0.5, 1, or 5 μ g/mL did not affect cell viability (**Figure 1A**). The migratory functions and capillary network formation of endothelial cells are believed to be important issues during atherogenesis. Therefore, *in vitro* wound-healing and tube formation assays were performed. After 24 hours of culture, the migratory ability decreased in 0.5, 1, and 5 μ g/mL GroEL-stimulated HCAECs (0.5 μ g/mL GroEL: 21.7 \pm 10.4% of the control, 1.0 μ g/mL GroEL: 204 \pm 6.7% of the control, and 19.7 \pm 9.4% of the control) (**Figure 1B**). After 24 hours of culture in 1 or 5 μ g/mL GroEL, the functional capacity for tube formation of HCAECs on ECMatrix gel was significantly decreased compared to the control group (1.0 μ g/mL GroEL: 70.5 \pm 8.2% of the control, and 52.3 \pm 7.2% of the control) (**Figure 1C**). These results indicate that GroEL (approximately 0.5-5 μ g/mL) potentially decreases the migra-

tion and tube formation capacity of HCAECs, which are involved in the lining of endothelium, whereas GroEL did not induce endothelial cell cytotoxicity.

GroEL increased HAEC/THP-1 cell adhesion in association with the expression of ICAM-1 and VCAM-1: The expression of adhesion molecules such as ICAM-1, VCAM-1, and E-selectin plays critical roles in the initial process during atherogenesis. Therefore, HCAEC/THP-1 cell adhesion assays were performed to analyze the effects of GroEL. In **Figure 2A**, the confluent control HCAECs showed minimal adhesiveness to THP-1 cells, but adhesion was substantially increased when the HCAECs were treated with 0.5, 1 or 5 μ g/mL of GroEL for 24 hour (152.7 \pm 20.1% of the control, 206.9 \pm 22.4% of the control, and 453.1 \pm 39.7% of the control, respectively). Adhesion molecules mediate the adhesion of monocytes to the endothelium; we predicted that VCAM-1 and ICAM-1 on endothelial cells may be involved in this process. The treatment of HCAECs with 10 μ g/mL of goat anti-hVCAM-1 or anti-hICAM-1 antibody before 5 μ g/mL GroEL treatment significantly reduced the adhesion of THP-1 cells (**Figure 2B**). In contrast, pretreatment of HCAECs with goat anti-hE-selectin antibody did not reduce the adhesion of THP-1 cells to GroEL-stimulated HCAECs. These results indicate that GroEL induces HCAEC/THP-1 cell adhesion. Furthermore, we predicted that the pheromone was mediated by adhesion molecule expression.

To confirm these findings, western blot analysis was performed (**Figure 2C**). ICAM-1, VCAM-1, and E-selectin were spontaneously expressed at a basal level in the control (untreated) HCAECs. GroEL treatment for 8 hours caused significant up-regulation of the expression of VCAM-1 and ICAM-1 but not E-selectin.

GroEL affects Dil-oxLDL uptake capacity mediated by LOX-1 and enhances LOX-1 expression in HCAECs: OxLDL induces inflammatory responses in endothelial cells. Therefore, a Dil-labeled oxLDL uptake assay was performed to investigate whether oxLDL uptake is enhanced in GroEL-stimulated HCAECs. Confocal microscopy demonstrated that treatment with 5 μ g/mL of GroEL for 24 hours significantly increased Dil-labeled oxLDL uptake by HCAECs (**Figure 3A**). Additionally, LOX-1, SREC and SR-B1 were

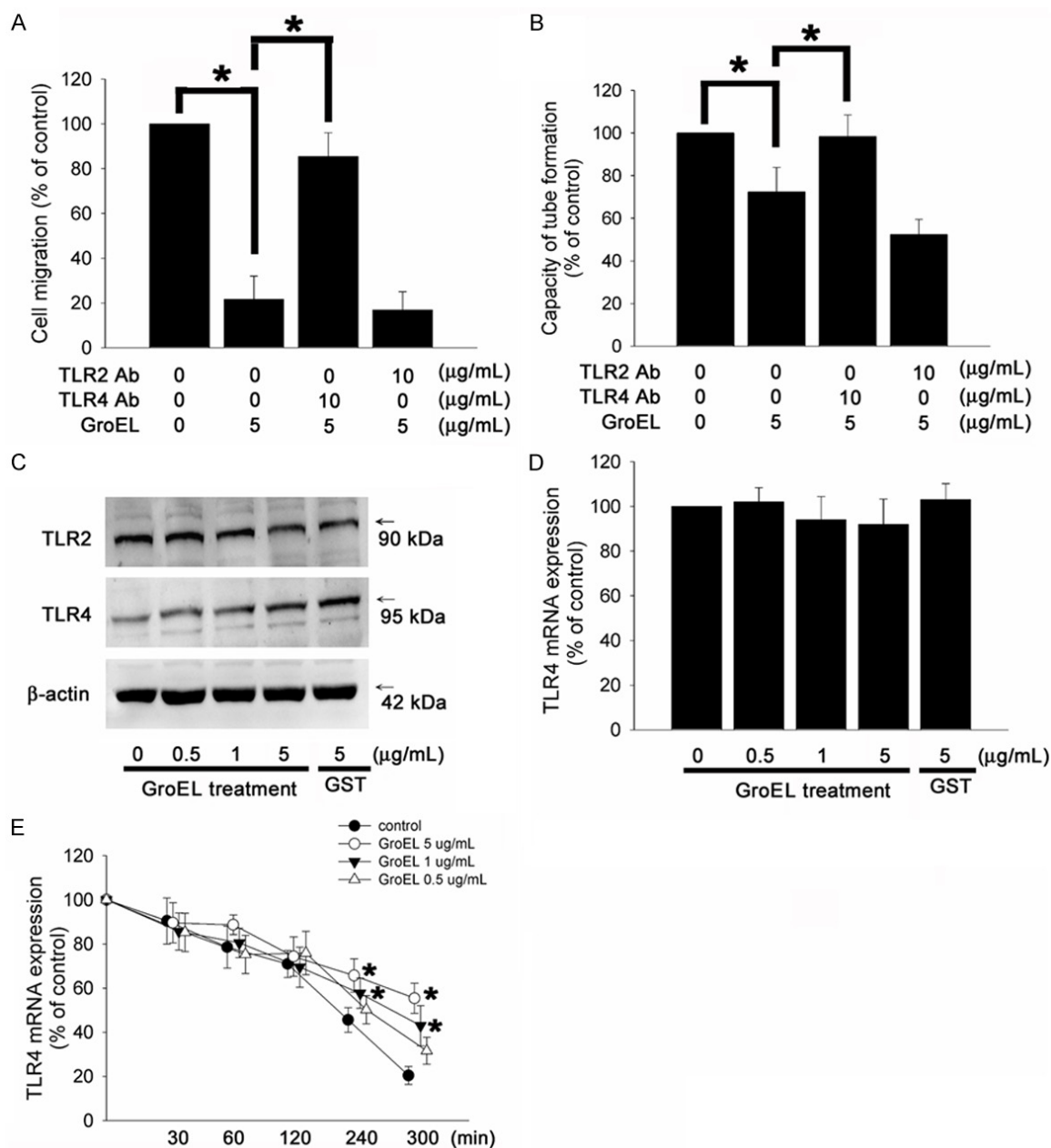


Figure 4. GroEL affects cell function mediated by TLR4 and enhances TLR4 mRNA stability in HCAECs. A, B. HCAECs were pretreated with 10 µg/mL anti-hTLR4 or anti-hTLR2 antibody for 1 hour prior to 5 µg/mL GroEL treatment for 24 hours. Wound-healing and tube formation assays were performed. The data are presented as the mean ± SD and represent the results from three independent experiments. Statistical evaluation was performed using one-way ANOVA followed by a Dunnett's test. * $P < 0.05$ was considered significant. * $p < 0.05$ was considered significant. C. HCAECs were treated with 0.5-5 µg/mL GroEL for 8 hours, TLR4 and TLR2 protein expression were analyzed by western blot analysis. D. HCAECs were treated with 0.5-5 µg/mL GroEL for 4 hours, TLR4 mRNA levels were analyzed by real-time PCR. Treatment with 5 µg/mL GST was used as a negative control. All bars represent the results of three independent experiments. The data are presented as the mean ± SD and statistical evaluation was performed using one-way ANOVA followed by a Dunnett's test. * $P < 0.05$ was considered significant. E. The half-life and level of TLR4 mRNA were analyzed by an actinomycin D chase experiment and quantitative real time PCR, respectively. The half-life of TLR4 mRNA was calculated according to the mRNA decay rate. The data are presented as the mean ± SD and represent the results from three independent experiments. Statistical evaluation was performed using one-way ANOVA followed by a Dunnett's test. * $P < 0.05$ was considered significant. * $p < 0.05$ compared to the control group in the same analysis time point was considered significant.

Porphyromonas gingivalis regulates atherogenesis

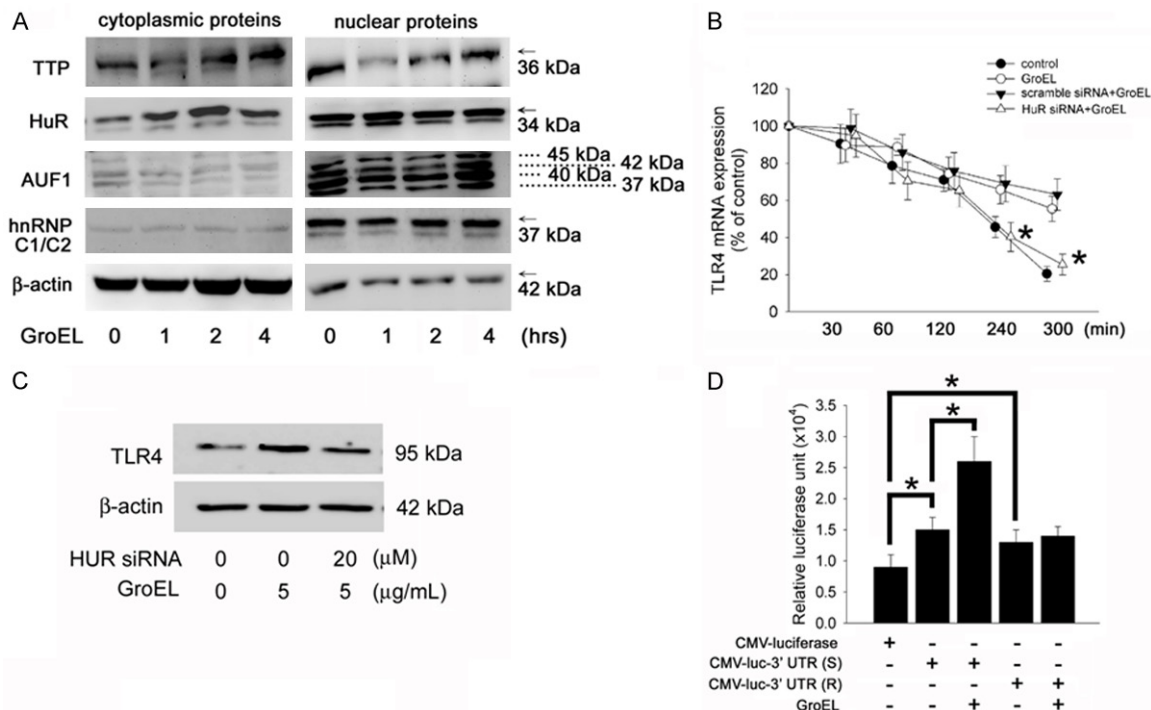


Figure 5. The 3'UTR of TLR4 mRNA confers GroEL responsiveness, and HuR modulates 3'UTR-mediated gene expression in HCAECs. **A.** HCAECs were treated with 5 μg/mL GroEL for 0-4 hours, and TTP, HuR and AUF1 protein expression in the cytoplasm and nucleus were analyzed using western blotting. hnRNP C1/C2 and β-actin and were used as internal controls. **B.** HuR in HCAECs was silenced by siRNA. The stability of TLR4 mRNA was analyzed by an actinomycin D chase experiment. The data are presented as the mean ± SD and represent the results from four independent experiments. Statistical evaluation was performed using one-way ANOVA followed by a Dunnett's test. *p<0.05 compared with the GroEL-treatment group in the same analysis time point was considered significant. **C.** HCAECs were treated with 20 μM HuR siRNA prior to 5 μg/mL GroEL for 8 hours, TLR4 protein expression were analyzed by western blot analysis. **D.** HCAECs were transfected with CMV-Luciferase-TLR4 3'UTR sense or CMV-Luciferase-TLR4 3'UTR antisense plasmid. An equal amount of a luciferase reporter gene containing plasmid (CMV-Luciferase) was used as a control. Uniform transfection efficiency was confirmed using a β-galactosidase reporter plasmid. The luciferase activity was quantified by luminometry. Data are expressed as relative luciferase units. The data are presented as the mean ± SD and represent the results from three independent experiments. Statistical evaluation was performed using one-way ANOVA followed by a Dunnett's test. *P<0.05 was considered significant.

originally identified on the membrane of vascular endothelial cells and are responsible for the uptake of LDL. The treatment of HCAECs with 10 μg/mL of goat anti-hLOX-1 but not rabbit anti-hSR-B1 or anti-hSREC antibody before 5 μg/mL GroEL treatment significantly reduced the uptake of Dil-labeled oxLDL by HCAECs. Western blotting showed that GroEL protein elevated membrane LOX-1 but not SE-B1 or SREC expression in HCAECs (**Figure 3B**).

GroEL affects cell functions mediated by TLR4 and enhances TLR4 expression in HCAECs: *P. gingivalis* mediates inflammation via TLR2 and TLR4 [31, 32]. Therefore, we studied the potency of TLR2 and TLR4 in GroEL-stimulated HCAECs. As shown in **Figure 4A**, mouse anti-hTLR4 antibody but not mouse anti-hTLR2 anti-

body (10 μg/mL) and subsequent incubation for 60 minutes prior to GroEL treatment for 24 hours significantly reversed the reduction of cell migration in GroEL-stimulated HCAECs. As a negative control in the competition assay, a nonspecific IgG2α isotype antibody was substituted for the TLR4-specific antibody; however, the nonspecific antibody did not affect GroEL-inhibited cell migration (data not shown). Similarly to **Figure 4A**, mouse anti-hTLR4 but not anti-hTLR2 antibody blocked the decrease of tube formation capacity in GroEL-stimulated HCAECs (**Figure 4B**). These results suggest the GroEL-decreased cell function in HCAECs is mediated by TLR4. In addition, treatment with GroEL protein for 8 hours significantly induced intracellular TLR4 expression, while in contrast decreasing TLR2 expression (**Figure 4C**). How-

ever, the total TLR4 mRNA level did not change under GroEL-stimulated conditions (**Figure 4D**). Our previous evidence demonstrated that the pathogen prolongs TLR4 mRNA stability, subsequently promoting TLR4 expression in vascular cells [30]. Therefore, an actinomycin D chase experiment was performed. HCAECs were treated with 0.5-5 $\mu\text{g}/\text{mL}$ GroEL for 4 hours and then actinomycin D for 1 hour. The $t_{1/2}$ of mRNA deduced for the various conditions indicated that GroEL stimulation rapidly increased the stability (half-life) of TLR4 mRNA in HCAECs (0.5 $\mu\text{g}/\text{mL}$ GroEL group (Δ): 275.7 \pm 30.2 minutes, 1 $\mu\text{g}/\text{mL}$ GroEL group (∇): 299.2 \pm 16.2 minutes, 5 $\mu\text{g}/\text{mL}$ GroEL group (\circ): more than 300 minutes, and control group (\bullet): 221.9 \pm 18.4 minutes) (**Figure 4D**). These results suggest that GroEL significantly induces TLR4 mRNA stability via post-transcriptional modification, which results in increased TLR4 expression in HCAECs.

GroEL triggers an increase in cytoplasmic HuR and prolongs TLR4 mRNA stability in HCAECs: TLR4 mRNA stability is regulated by AU-rich element (ARE)/RNA binding proteins such as human antigen R (HuR), AU binding factor 1 (AUF 1), and tristetraprolin (TTP) in vascular cells [30, 33]. Therefore, western blotting was performed to analyze the distribution/activation of HuR, AUF1, and TTP. Treatment with 5 $\mu\text{g}/\text{mL}$ GroEL caused a marked accumulation of cytoplasmic HuR and TTP over time (1-4 hours) (**Figure 5A**); in contrast, AUF1 expression was found predominantly in the nucleus, and its distribution remained unchanged following GroEL treatment. The level of nuclear HuR did not decrease concomitantly with the increase in cytoplasmic HuR. Heterogeneous nuclear ribonucleoprotein (hnRNP) C1/C2 and β -actin were used to monitor the process of protein extraction, and the extracted protein was loaded on gels. GroEL-prolonged TLR4 mRNA stability (\circ) was completely blocked by HuR siRNA (Δ) (**Figure 5B**); this effect was not observed with scrambled siRNA (∇), suggesting a critical role of HuR in the regulation of TLR4 mRNA stability. Additionally, treatment with HuR siRNA prior to 5 $\mu\text{g}/\text{mL}$ GroEL protein for 8 hours significantly reversed the induction of intracellular TLR4 expression in HCAECs (**Figure 5C**). Based on the cytoplasmic localization of HuR in endotoxin-treated smooth muscle cells and the specific region of ARE recog-

nized by HuR [34], we demonstrated that HuR interacts with the 3'UTR of TLR4 mRNA [30]. To investigate whether the 3'UTR promotes TLR4 mRNA expression in GroEL-stimulated HCAECs, a reporter plasmid containing the 3'UTR and a luciferase reporter gene was transfected into cells. The CMV-Luciferase-TLR4 3'UTR sense and CMV-Luciferase-TLR4 3'UTR antisense plasmid-transfected groups had higher basal luciferase activity than the CMV-Luciferase plasmid-transfected group. Treatment with 5 $\mu\text{g}/\text{mL}$ LPS caused a significant increase in luciferase activity in the CMV-Luciferase-TLR4 3'UTR sense plasmid-transfected group. In contrast, GroEL treatment did not change the basal luciferase activity in the CMV-Luciferase-TLR4 3'UTR antisense plasmid-transfected group (**Figure 5D**). These observations suggest that the 3'UTR of TLR4 mRNA confers GroEL responsiveness and that HuR modulates the 3'UTR-mediated gene expression in HCAECs.

Animal study

Biochemical measurements of experimental mice: As shown in **Table 1**, during the experimental period, weight gain and final weight did not differ significantly between the groups of animals.

The serum levels of indicators for kidney function (BUN, normal range 18-29 mg/dL and creatinine, normal range 0.2-0.8 mg/dL) and liver function (ALT, normal range 59-247 IU/L and AST, normal range 28-132 IU/L) also showed no significant difference between groups. Additionally, LDH is an enzyme found in living animal cells that is released during tissue damage such as cardiovascular disease. Compared to the control group, neither the HC diet nor GroEL protein treatment affected the serum LDH level significantly in any group at the same time point during the experimental period.

GroEL accelerates the increase of serum lipid levels in mice: The levels of total-cholesterol, TG, HDL, and LDL are shown in **Table 2**. During the experimental period, the levels of total-cholesterol, TG, HDL, and LDL did not differ significantly in wild C57BL/6 and C57BL/6-*Tlr4*^{lps-del} mice fed the normal chow diet. Feeding the HC diet to wild C57BL/6 or C57BL/6-*Tlr4*^{lps-del} mice may effectively increase levels of total-cholesterol, TG, and LDL in a time-dependent manner ($^{\#}p<0.05$ compared with week 0 in the same

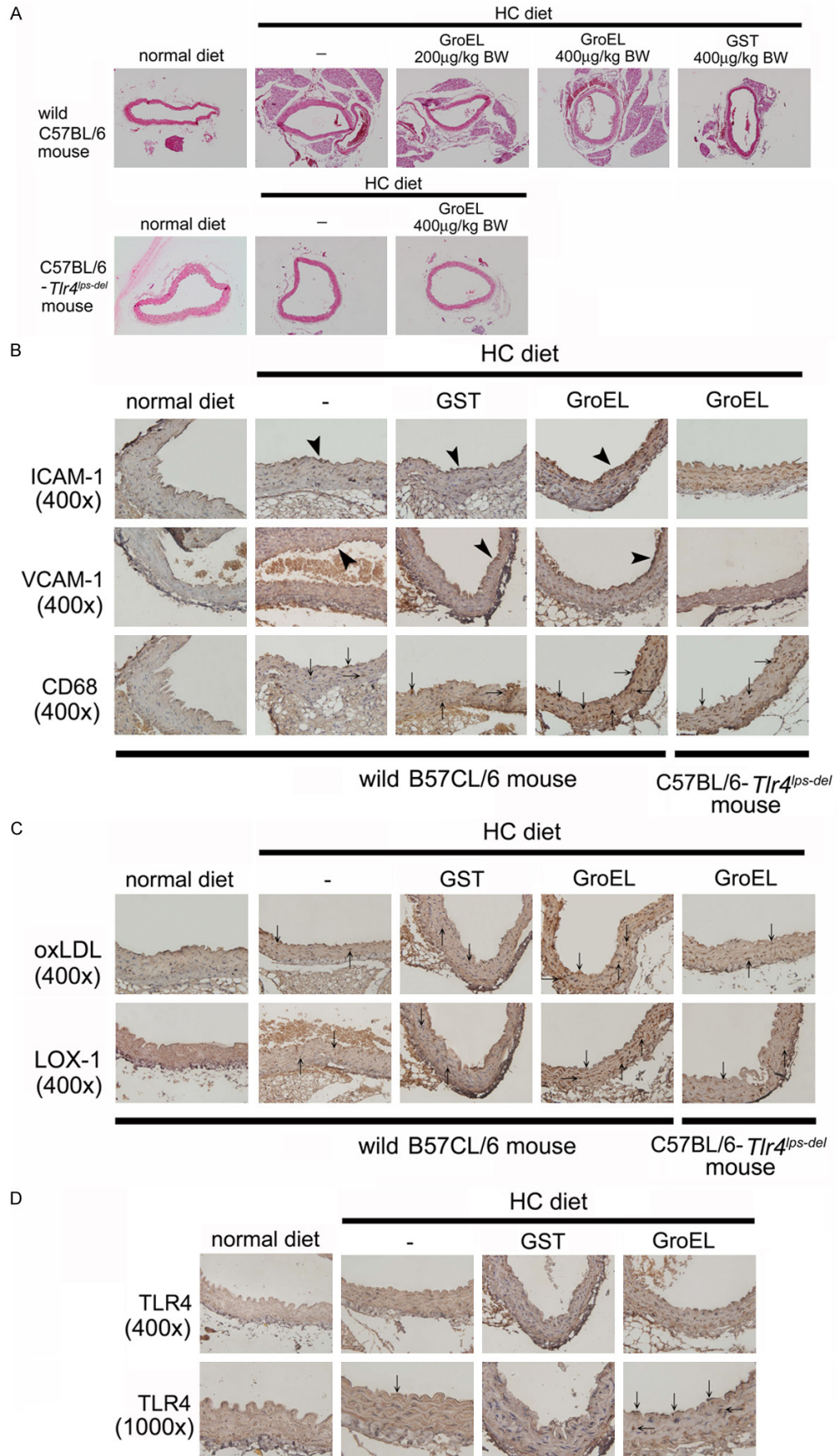
Porphyromonas gingivalis regulates atherogenesis

Table 2. Plasma lipid profiles (n=5) in experimental mice

	wk	Wild C57BL/6 mouse					C57BL/6- <i>Tlr4</i> ^{lps-def} mouse		
		Normal diet		HC diet			Normal diet		HC diet
		-	-	GroEL 200 µg/kg BW	GroEL 400 µg/kg BW	GST 400 µg/kg BW	-	-	GroEL 400 µg/kg BW
t-Cho (mg/dL)	0	105.4±5.0	97.4±9.7	96.2±8.5	114.0±11.5	91.3±8.2	99.6±5.9	72.1±4.6	105.7±6.9
	2	103.5±4.6	369.6±28.2 ^a	615.2±48.5 ^{a,c}	595.8±33.5 ^{a,c}	426.0±73.5 ^a	108.9±9.7	343.2±56.9 ^a	416.3±55.0 ^{a,d}
	4	94.4±4.5	665.1±78.1 ^{a,b}	761.9±85.1 ^{a,b}	639.3±16.8 ^a	660.4±55.2 ^{a,b}	100.5±9.7	452.1±53.8 ^{a,b}	645.3±77.0 ^{a,b}
TG (mg/dL)	0	64.5±7.5	76.0±6.2	70.0±21.5	60.3±25.9	60.3±6.4	53.9±8.4	50.1±6.5	56.0±18.8
	2	66.9±6.4	107.3±9.8 ^a	144.8±33.5 ^{a,c}	162.5±35.1 ^{a,c}	121.3±8.0 ^a	45.3±16.5	145.2±30.9 ^a	140.7±25.3 ^a
	4	67.5±6.5	182.0±33.6 ^{a,b}	267.3±22.8 ^{a,b,c}	269.5±35.5 ^{a,b,c}	186.0±32.8 ^{a,b}	35.6±19.1	253.2±26.1 ^{a,b}	236.0±34.9 ^{a,b}
HDL (mg/dL)	0	42.4±14.2	59.8±5.4	56.6±9.2	53.5±14.2	53.6±14.2	40.2±13.8	52.1±13.6	42.7±18.7
	2	49.4±13.2	77.7±16.1	76.7±11.3	56.7±8.2	72.8±12.2	49.8±15.4	48.9±6.4	42.0±14.5
	4	41.8±14.2	79.6±7.2	69.7±10.2	62.6±7.4	63.6±16.2	44.6±9.1	44.2±16.1	45.3±15.3
LDL (mg/dL)	0	55.8±17.4	44.4±11.9	56.9±6.9	49.8±13.2	59.9±6.7	52.3±5.4	41.6±7.5	42.3±4.5
	2	41.1±11.2	271.9±27.9 ^a	510.3±53.6 ^{a,c}	507.7±35.6 ^{a,c}	330.5±81.3 ^a	31.2±6.8	242.8±89.1 ^a	346.0±49.7 ^{a,d}
	4	40.9±9.2	550.8±94.9 ^{a,b}	639.5±94.6 ^{a,b}	867.2±22.5 ^{a,b,c}	512.3±51.2 ^{a,b}	45.6±9.1	546.9±58.7 ^{a,b}	637.7±79.8 ^{a,b,d}

t-Cho, total-cholesterol; TG, triglyceride; HDL, high density lipoprotein; LDL, low density lipoprotein. Values are mean ± SD. ^ap<0.05 compared with 0 week at the same group; ^bp<0.05 compared with 2 week at the same group; ^cp<0.05 compared with group 2 (wild type C57BL/6 mice fed with HC diet) at the same time point; ^dp<0.05 compared with group 4 (wild type C57BL/6 mice fed with HC diet and received 400 µg/kg BW of GroEL) at the same time point.

Porphyromonas gingivalis regulates atherogenesis



Porphyromonas gingivalis regulates atherogenesis

Figure 6. GroEL protein induces atherosclerotic factor expression in HC diet-fed mice, which is mediated by TLR4 expression in C57BL/6 mice. A. Histopathological features of cross-sections of aortas were stained using hematoxylin and eosin. There were no atherosclerotic lesions in the aortas of any group. The graphs show 100x magnification of the slide. B-D. Immunohistochemistry to assess ICAM-1, VCAM-1, infiltrated monocytic cells (CD68), oxLDL, LOX-1, and TLR4 in mouse aortas. The lumen is uppermost in all sections, and corresponding hematoxylin staining was used to identify the nucleus. The graphs show 400x or 1000x magnification of the slide.

group, and $^b p < 0.05$ compared with week 2 in the same group). Levels of total-cholesterol, TG, and LDL reached 665.1 ± 78.1 mg/dL, 182.0 ± 33.6 mg/dL, and 550.8 ± 94.8 mg/dL, respectively, in wild C57BL/6 mice fed the HC diet before sacrifice at the end of experiment. Similarly, levels of total-cholesterol reached 452.1 ± 53.8 mg/dL, TG reached 253.2 ± 26.1 mg/dL, and LDL reached 546.9 ± 58.7 mg/dL in C57BL/6-*Tlr4*^{lps-/-} mice fed the HC diet at the end of the experiment. HC diet-fed wild C57BL/6 mice receiving 200 μ g/kg BW or 400 μ g/kg BW of GroEL also experienced elevation of total-cholesterol, TG, and LDL. Interestingly, significant differences in total-cholesterol levels between GroEL-treated plus HC diet-fed wild C57BL/6 mice and only HC diet-fed wild C57BL/6 mice were observed at the 2nd week of the experimental period ($^c p < 0.05$ compared with wild C57BL/6 mice fed with HC diet), even though no significant difference was observed at the 4th week of the experimental period. This result indicated that GroEL may accelerate the increase of serum total-cholesterol levels. Additionally, injection of GroEL may accelerate the increase of serum TG and LDL levels and allow higher TG and LDL levels in HC diet-fed wild C57BL/6 mice when compared to only HC diet-fed wild C57BL/6 mice ($^c p < 0.05$ compared with wild C57BL/6 mice fed with HC diet at the same time point). In contrast, these phenomena were not observed in C57BL/6-*Tlr4*^{lps-del} mice fed the HC diet ($^d p < 0.05$ compared with wild C57BL/6 mice fed with HC diet and receiving 400 μ g/kg BW of GroEL at the same time point). These results indicated that GroEL may enhance atherosclerotic risk factors such as TG and LDL in serum, which is mediated by TLR4-related axis mechanisms.

GroEL enhances adhesion molecule and LOX-1 expression and induces cell accumulation in HC Diet-fed C57BL/6 But Not C57BL/6-Tlr4^{lps-del} mice: Representative photographs of aortas stained with hematoxylin and eosin from C57BL/6 and C57BL/6-*Tlr4*^{lps-del} mice are shown in **Figure 6A**. There was no thickened intima

or atherosclerotic lesion formation in the aortas of either C57BL/6 or C57BL/6-*Tlr4*^{lps-del} mice. Adhesion molecules, especially ICAM-1 and VCAM-1, play critical roles in atherogenesis. Therefore, immunohistochemical staining was performed using antibodies against VCAM-1 and ICAM-1 on sections of the aortas (**Figure 6B**). Compared with sections from the control (normal diet) group, the sections of the wild C57BL/6 mouse aortas showed slightly increased ICAM-1 and VCAM-1 expression on the endothelium and luminal surface in the HC diet-fed and HC diet+ GST (400 μ g/kg BW) treatment groups (black arrow heads). Indeed, treatment with GroEL (400 μ g/kg BW) strengthened ICAM-1 and VCAM-1 expression in the HC diet-fed group. Obviously, GroEL administration did not increase ICAM-1 or VCAM-1 expression in the aortas of the HC diet-fed C57BL/6-*Tlr4*^{lps-del} mice. Staining with the anti-CD68 antibody to identify infiltrated macrophages showed that fewer macrophages infiltrated into the vessel walls in the normal diet-fed group, and there were fewer macrophages in the HC diet-fed and HC diet+GST treatment groups compared with the HC diet+GroEL group in wild C57BL/6 mice (black arrows). Although the 400 μ g/kg BW GroEL group did exhibit increased macrophage infiltration, there was more severe macrophage infiltration in the HC diet-fed C57BL/6-*Tlr4*^{lps-del} mice. Additionally, compared with sections from the non-GroEL treatment groups, the administration of 400 μ g/kg BW GroEL enhanced oxLDL accumulation/form cell formation in the vessels of the HC diet-fed C57BL/6 mice. **Figure 6C** shows antibodies against LOX-1 on sections of the aortas. Compared with sections from the normal diet-fed group, slightly enhanced LOX-1 expression appeared in the vessel walls of the HC diet-fed C57BL/6 mice both with and without GST administration (black arrows). Similarly to **Figure 6B**, there was no increase of LOX-1 expression in the HC diet-fed C57BL/6-*Tlr4*^{lps-del} mice when compared with wild C57BL/6 mice. In contrast, GroEL administration induced neither SREC nor SR-B1 expression in the aorta in C57BL/6 mice

(Supplementary Figure 1). These results demonstrate that GroEL administration significantly exacerbated atherosclerotic gene expression in the aorta in HC diet-fed C57BL/6 mice, as mediated by TLR4. Finally, according to the results *in vitro* that GroEL induces TLR4 expression in HCAECs, and *in vivo* that GroEL enhances adhesion molecule (VCAM-1 and ICAM-1) and LOX-1 expression in HC diet-fed wild C57BL/6 but not C57BL/6-*Tlr4^{lps-del}* mice, we analyzed TLR4 expression in GroEL treated mice.

Figure 6D shows that a very slight increase of TLR4 expression was observed on the vessel endothelium only in the HC diet-fed and GST treatment+HC diet-fed B57CL/6 mice compared to the normal diet groups. The combination of GroEL (400 µg/kg BW) treatment and the HC diet may prove that the TLR4 expression is increased (black arrows). To combine these findings, GroEL administration increased ICAM-1, VCAM-1, and LOX-1 expression in mouse vessels, and this was mediated by TLR4.

Discussion

GroEL from *P. gingivalis* impaired HCAEC function and induced VCAM-1, ICAM-1, LOX-1 expression, which mediates monocyte adhesion and infiltration. Additionally, TLR4 plays a causal role in GroEL-induced inflammatory responses in HCAECs. HuR has high affinity for the 3'UTR of TLR4 mRNA to prolong its stability, which contributes to the up-regulation of TLR4 in GroEL-stimulated HCAECs. Similarly, GroEL enhanced the levels of TG and LDL in serum, increased ICAM-1, VCAM-1, LOX-1, and TLR4 expression, and increased monocyte infiltration in aortas of hypercholesterolemic wild C57BL/6 but not C57BL/6-*Tlr4^{lps-del}* mice. The data provide evidence for the direct involvement of GroEL, which may mediate the progression of atherosclerosis.

Previous evidence had demonstrated that *P. gingivalis*, in addition to inducing periodontal diseases, also exacerbates many systemic diseases in human beings [35-37], such as atheroma, atherosclerosis, arterial thrombus, abdominal aneurysm, and varicose veins, etc. However, LPS from *P. gingivalis* is known to be a major component that induces vascular inflammation. LPS from *P. gingivalis* induces angiogenesis [38]; increases expression of granu-

locyte-macrophage colony-stimulating factor (GM-CSF), monocyte chemoattractant protein-1 (MCP-1), interleukin (IL)-1b, IL-10, and IL-12 in oxLDL-stimulated form cells [39]; induces inflammasome activation in macrophages [40]; and activates cathepsin [41] and VCAM-1 [42] expression in endothelial cells. Additionally, gingipain from *P. gingivalis* is recognized by natural IgM and shares molecular identity with malondialdehyde modified-LDL, which is associated with atherogenesis [43]. Different from other teams' research, our group's investigations have focused on the effects of GroEL from *P. gingivalis* on systemic inflammation. Recently, we presented that GroEL of *P. gingivalis* accelerates tumor growth by enhancing endothelial progenitor cell function and neovascularization [44]. TLR2 and TLR4 are critical for the induction of downstream signals in cardiovascular diseases [45]. Scientists have acquired evidence that *P. gingivalis* enhances monocyte migration and cytokine production [46] and exacerbates endothelial cell injury [47-50], and TLR2 and TLR 4 jointly play critical roles in *P. gingivalis*-mediated inflammatory atherosclerosis [31, 32]. Although previous findings implicated lipopolysaccharide LPS and the pro-atherogenic advanced glycation end products (AGEs) signaling axis [51] associated with *P. gingivalis*-mediated vascular functional disturbances, the present findings indicate for the first time the roles of GroEL in the pro-atherogenic responses in vascular endothelial cells. Additionally, although *P. gingivalis* LPS may confer cardioprotection during ischemia and reperfusion [52], and TLR4 signaling may play protective roles in oral pathogen-induced atherosclerosis progression [53], the actual critical roles of TLR4 still need to be elucidated in the highly variable and dynamic atherogenesis induced by *P. gingivalis*. Infection by *P. gingivalis* significantly induces the expression of TLR4 and TLR2 in mice regardless of whether hyperlipidemia is present [54]. GroEL induces its intracellular signaling via a combination of both TLR4 and TLR2 in monocytic THP-1 cells [25]. The identity of the components from *P. gingivalis* involved in TLR2 signaling and mediating atherosclerosis also need to be studied.

In general, the accumulation of atherosclerotic atheroma/plaque is difficult to observe in mice lacking deficiencies of lipid-metabolic genes, such as apolipoprotein E and LDL receptor, in a

short duration HC diet treatment (4 weeks for this experiment) [54]. Therefore, in this study, we used wild C57BL/6 mice in order to analyze the biological effects of GroEL on lipid profile metabolism and vascular function under normal physiological conditions. Indeed, HC diet-fed wild C57CL/B6 mice receiving GroEL also experienced an accelerated increase of serum total-cholesterol, TG, and LDL levels. Maekawa *et al.* had also presented that chronic oral infection with *P. gingivalis* accelerates atheroma formation by changing cholesterol transport and shifting the lipid profile [54]. In contrast, *P. gingivalis* induced slightly higher levels of total cholesterol, TG, LDL, and HDL that did not, however, reach significance. However, long-term (24 weeks) infection leads to elevated levels of oxidized LDL in mice [55]. A limitation of the animal model is the relatively short duration of the HC diet and *P. gingivalis* infection. The species differences between humans and mice are the key issue that needs to be studied. Furthermore, LDL affects the cytokine responses of macrophages to *P. gingivalis* challenge, and TLR4-MyD88 signaling plays important roles in *P. gingivalis*-elicited foam cell formation [56]. In our *in vitro* and *in vivo* studies, GroEL induced endothelial cell inflammation and functional disturbances *via* TLR4; GroEL also enhanced TLR4 expression on vessel walls. We predict that increased presence of TLR4 on vessel walls is likely to cause the hypersensitivity of vascular cells to GroEL, and so exacerbate and worsen the inflammation. Nevertheless, administration of GroEL may accelerate the increase of serum TG and LDL levels and allow higher TG and LDL levels in HC diet-fed wild C57CL/B6 mice, but not C57BL/6-*Tlr4*^{lps-/-} mice; there is scant evidence exploring the mechanisms by which the TLR4-related axis modulates the profile of lipid metabolism in animals.

Much evidence has revealed an association between periodontitis and cancers such as non-Hodgkin lymphoma [6], metastatic pancreatic cancer [57], lung cancer [58], osteogenic sarcoma [59], gastric cancer [6, 60, 61], and esophageal cancer [61]. Recent results of our group showed that GroEL of *P. gingivalis* accelerates tumor growth by enhancing endothelial progenitor cell (EPC) mobilization, differentiation, function and neovascularization, which is mediated by eNOS production and p38 mitogen-activated protein kinase (MAPK) activation

[44]. Moreover, EPCs play a critical role of repairing vascular site damage during atherogenesis. However, because of the dissimilar intracellular regulation involved in EPC-associated atherosclerosis and neovascularization, and the typical/common mouse models (HC diet fed-ApoE-deficient or -LDL receptor knock-out mice) for atherosclerosis research were not applied in the present study, therefore we could only observe the influence of GroEL-administration on atherogenic gene expression and not EPC function in mice. During the process of atherogenesis, whether GroEL indeed influences the function of EPCs is worth further exploration. M. Hagiwara *et al.* suggested that sublingual immunization with recombinant GroEL is associated with a systemic humoral response, which could be a strategy for *P. gingivalis*-related atherosclerosis [62]. Recently, E. Jeong's group identified the use of a Pep 14-specific Tregs-based T-cell vaccine to suppress atherogenesis [63]. Although the mechanisms and causes of atherosclerosis resulting from GroEL of *P. gingivalis* are still unclear, devising a GroEL-based vaccine may be a feasible strategy to prevent *P. gingivalis*-associated arteriosclerosis and tumorigenesis.

Efficient adjustment of inflammatory responses may occur via control of mRNA stability to modulate gene expression. Through the interaction of RNA binding proteins such as HuR, AUF 1, and tristetraprolin (TTP) [33] with AREs of 3'UTRs, the stability of mRNA is often modulated [64]. HuR stabilizes mRNAs of thrombomodulin [65], TLR4 [30], c-Fos, granulocyte macrophage colony stimulating factor (GM-CSF), TNF- α [34, 66, 67], COX-2 [68], cyclins [69], and p21 [70]. Presently, our data revealed that HuR binds to the ARE of TLR4 mRNA, interacting directly with the 3'UTR to prolong the mRNA's stability in GroEL-stimulated HCAECs. The data provide evidence for the direct involvement of HCAECs in GroEL-mediated TLR4 expression, which may contribute to the progression of cardiovascular disorders. TTP is a zinc finger protein and has been critically implicated in inflammation. TTP are countered by HuR [71]; TTP destabilizes TLR4 [72], thrombomodulin [65], TNF- α [73], GM-CSF [74], and IL-3 [75] mRNA. Knockout of TTP may cause a severe inflammatory syndrome *in vivo* [76], and up-regulation of TTP on monocytes resulting from cardiac surgery may induce immune sup-

pression via regulation of TLR4 expression [65]. AUF1 exists in four isoforms (p37^{AUF1}, p40^{AUF1}, p42^{AUF1}, and p45^{AUF1}). The activation of AUF1 causes diverse impacts on mRNA stability during inflammation. Our work identified TLR4 as a target gene for GroEL. This provides a basis for further investigation of TLR4 modulation as a therapeutic strategy for atherogenesis in *P. gingivalis* infection.

Acknowledgements

We thank Mr. Tze-Liang Yang and Mrs. Min-Yu Lo for excellent technical assistance. This work was supported by National Ministry of Science and Technology (NSC 101-2314-B-038 -041-MY3 and MOST 104-2314-B-038-072) and Taipei Medical University (103TMU-TMUH-10) in Taiwan.

Disclosure of conflict of interest

The author(s) confirm that this article content has no conflicts of interest.

Address correspondence to: Dr. Feng-Yen Lin, Department of Internal Medicine, School of Medicine, College of Medicine, Taipei Medical University, Taipei City, 110 Taiwan. E-mail: g870905@tmu.edu.tw

References

- [1] Chung SW, Kang HS, Park HR, Kim SJ, Kim SJ and Choi JI. Immune responses to heat shock protein in *Porphyromonas gingivalis*-infected periodontitis and atherosclerosis patients. *J Periodontol Res* 2003; 38: 388-393.
- [2] Tabeta K, Yamazaki K, Hotokezaka H, Yoshie H and Hara K. Elevated humoral immune response to heat shock protein 60 (hsp60) family in periodontitis patients. *Clin Exp Immunol* 2000; 120: 285-293.
- [3] Malek R, Fisher JG, Caleca A, Stinson M, van Oss CJ, Lee JY, Cho MI, Genco RJ, Evans RT and Dyer DW. Inactivation of the *Porphyromonas gingivalis* fimA gene blocks periodontal damage in gnotobiotic rats. *J Bacteriol* 1994; 176: 1052-1059.
- [4] Reife RA, Shapiro RA, Bamber BA, Berry KK, Mick GE and Darveau RP. *Porphyromonas gingivalis* lipopolysaccharide is poorly recognized by molecular components of innate host defense in a mouse model of early inflammation. *Infect Immun* 1995; 63: 4686-4694.
- [5] Hayashi C, Gudino CV, Gibson FC 3rd and Genco CA. Review: Pathogen-induced inflammation at sites distant from oral infection: bacterial persistence and induction of cell-specific innate immune inflammatory pathways. *Mol Oral Microbiol* 2010; 25: 305-316.
- [6] Michaud DS, Liu Y, Meyer M, Giovannucci E and Joshipura K. Periodontal disease, tooth loss, and cancer risk in male health professionals: a prospective cohort study. *Lancet Oncol* 2008; 9: 550-558.
- [7] Picolos DK, Lerche-Sehm J, Abron A, Fine JB and Papapanou PN. Infection patterns in chronic and aggressive periodontitis. *J Clin Periodontol* 2005; 32: 1055-1061.
- [8] Ezzo PJ and Cutler CW. Microorganisms as risk indicators for periodontal disease. *Periodontol* 2000 2003; 32: 24-35.
- [9] Lamont RJ and Jenkinson HF. Subgingival colonization by *Porphyromonas gingivalis*. *Oral Microbiol Immunol* 2000; 15: 341-349.
- [10] Katz J, Onate MD, Pauley KM, Bhattacharyya I and Cha S. Presence of *Porphyromonas gingivalis* in gingival squamous cell carcinoma. *Int J Oral Sci* 2011; 3: 209-215.
- [11] Hajishengallis G. *Porphyromonas gingivalis*-host interactions: open war or intelligent guerrilla tactics? *Microbes Infect* 2009; 11: 637-645.
- [12] Yilmaz O. The chronicles of *Porphyromonas gingivalis*: the microbium, the human oral epithelium and their interplay. *Microbiology* 2008; 154: 2897-2903.
- [13] Kuboniwa M, Hasegawa Y, Mao S, Shizukuishi S, Amano A, Lamont RJ and Yilmaz O. *P. gingivalis* accelerates gingival epithelial cell progression through the cell cycle. *Microbes Infect* 2008; 10: 122-128.
- [14] Maeda H, Miyamoto M, Kokeguchi S, Kono T, Nishimura F, Takashiba S and Murayama Y. Epitope mapping of heat shock protein 60 (GroEL) from *Porphyromonas gingivalis*. *FEMS Immunol Med Microbiol* 2000; 28: 219-224.
- [15] Ueki K, Tabeta K, Yoshie H and Yamazaki K. Self-heat shock protein 60 induces tumour necrosis factor-alpha in monocyte-derived macrophage: possible role in chronic inflammatory periodontal disease. *Clin Exp Immunol* 2002; 127: 72-77.
- [16] Retzlaff C, Yamamoto Y, Hoffman PS, Friedman H and Klein TW. Bacterial heat shock proteins directly induce cytokine mRNA and interleukin-1 secretion in macrophage cultures. *Infect Immun* 1994; 62: 5689-5693.
- [17] Tabona P, Reddi K, Khan S, Nair SP, Crean SJ, Meghji S, Wilson M, Preuss M, Miller AD, Poole S, Carne S and Henderson B. Homogeneous *Escherichia coli* chaperonin 60 induces IL-1 beta and IL-6 gene expression in human monocytes by a mechanism independent of protein conformation. *J Immunol* 1998; 161: 1414-1421.
- [18] Zhang Y, Doerfler M, Lee TC, Guillemin B and Rom WN. Mechanisms of stimulation of inter-

Porphyromonas gingivalis regulates atherogenesis

- leukin-1 beta and tumor necrosis factor-alpha by Mycobacterium tuberculosis components. *J Clin Invest* 1993; 91: 2076-2083.
- [19] Goulhen F, Hafezi A, Uitto VJ, Hinode D, Nakamura R, Grenier D and Mayrand D. Sub-cellular localization and cytotoxic activity of the GroEL-like protein isolated from *Actinobacillus actinomycetemcomitans*. *Infect Immun* 1998; 66: 5307-5313.
- [20] Hinode D, Yoshioka M, Tanabe S, Miki O, Masuda K and Nakamura R. The GroEL-like protein from *Campylobacter rectus*: immunological characterization and interleukin-6 and -8 induction in human gingival fibroblast. *FEMS Microbiol Lett* 1998; 167: 1-6.
- [21] Tanabe S, Hinode D, Yokoyama M, Fukui M, Nakamura R, Yoshioka M, Grenier D and Mayrand D. *Helicobacter pylori* and *Campylobacter rectus* share a common antigen. *Oral Microbiol Immunol* 2003; 18: 79-87.
- [22] Galdiero M, de l'Ero GC and Marcatili A. Cytokine and adhesion molecule expression in human monocytes and endothelial cells stimulated with bacterial heat shock proteins. *Infect Immun* 1997; 65: 699-707.
- [23] Verdegaal ME, Zegveld ST and van Furth R. Heat shock protein 65 induces CD62e, CD106, and CD54 on cultured human endothelial cells and increases their adhesiveness for monocytes and granulocytes. *J Immunol* 1996; 157: 369-376.
- [24] Lee JY, Yi NN, Kim US, Choi JS, Kim SJ and Choi JI. *Porphyromonas gingivalis* heat shock protein vaccine reduces the alveolar bone loss induced by multiple periodontopathogenic bacteria. *J Periodontal Res* 2006; 41: 10-14.
- [25] Argueta JG, Shiota S, Yamaguchi N, Masuhiro Y and Hanazawa S. Induction of *Porphyromonas gingivalis* GroEL signaling via binding to Toll-like receptors 2 and 4. *Oral Microbiol Immunol* 2006; 21: 245-251.
- [26] Chen JZ, Zhu JH, Wang XX, Xie XD, Sun J, Shang YP, Guo XG, Dai HM and Hu SJ. Effects of homocysteine on number and activity of endothelial progenitor cells from peripheral blood. *J Mol Cell Cardiol* 2004; 36: 233-239.
- [27] Hsu YT, Wolter KG and Youle RJ. Cytosol-to-membrane redistribution of Bax and Bcl-X(L) during apoptosis. *Proc Natl Acad Sci U S A* 1997; 94: 3668-3672.
- [28] Steinbrecher UP, Parthasarathy S, Leake DS, Witztum JL and Steinberg D. Modification of low density lipoprotein by endothelial cells involves lipid peroxidation and degradation of low density lipoprotein phospholipids. *Proc Natl Acad Sci U S A* 1984; 81: 3883-3887.
- [29] Lin FY, Lin YW, Huang CY, Chang YJ, Tsao NW, Chang NC, Ou KL, Chen TL, Shih CM and Chen YH. GroEL1, a heat shock protein 60 of *Chlamydia pneumoniae*, induces lectin-like oxidized low-density lipoprotein receptor 1 expression in endothelial cells and enhances atherogenesis in hypercholesterolemic rabbits. *J Immunol* 2011; 186: 4405-4414.
- [30] Lin FY, Chen YH, Lin YW, Tsai JS, Chen JW, Wang HJ, Chen YL, Li CY and Lin SJ. The role of human antigen R, an RNA-binding protein, in mediating the stabilization of toll-like receptor 4 mRNA induced by endotoxin: a novel mechanism involved in vascular inflammation. *Arterioscler Thromb Vasc Biol* 2006; 26: 2622-2629.
- [31] Hayashi C, Madrigal AG, Liu X, Ukai T, Goswami S, Gudino CV, Gibson FC 3rd and Genco CA. Pathogen-mediated inflammatory atherosclerosis is mediated in part via Toll-like receptor 2-induced inflammatory responses. *J Innate Immun* 2010; 2: 334-343.
- [32] Pan S, Lei L, Chen S, Li H and Yan F. Rosiglitazone impedes *Porphyromonas gingivalis*-accelerated atherosclerosis by downregulating the TLR/NF-kappaB signaling pathway in atherosclerotic mice. *Int Immunopharmacol* 2014; 23: 701-708.
- [33] Kracht M and Saklatvala J. Transcriptional and post-transcriptional control of gene expression in inflammation. *Cytokine* 2002; 20: 91-106.
- [34] Fan XC and Steitz JA. Overexpression of HuR, a nuclear-cytoplasmic shuttling protein, increases the in vivo stability of ARE-containing mRNAs. *EMBO J* 1998; 17: 3448-3460.
- [35] Inaba H and Amano A. Roles of oral bacteria in cardiovascular diseases—from molecular mechanisms to clinical cases: Implication of periodontal diseases in development of systemic diseases. *J Pharmacol Sci* 2010; 113: 103-109.
- [36] Iwai T. Periodontal bacteremia and various vascular diseases. *J Periodontal Res* 2009; 44: 689-694.
- [37] Amar S and Engelke M. Periodontal innate immune mechanisms relevant to atherosclerosis. *Mol Oral Microbiol* 2015; 30: 171-185.
- [38] Koo TH, Jun HO, Bae SK, Kim SR, Moon CP, Jeong SK, Kim WS, Kim GC, Jang HO, Yun I, Kim KW and Bae MK. *Porphyromonas gingivalis*, periodontal pathogen, lipopolysaccharide induces angiogenesis via extracellular signal-regulated kinase 1/2 activation in human vascular endothelial cells. *Arch Pharm Res* 2007; 30: 34-42.
- [39] Lei L, Li H, Yan F, Li Y and Xiao Y. *Porphyromonas gingivalis* lipopolysaccharide alters atherosclerotic-related gene expression in oxidized low-density-lipoprotein-induced macrophages and foam cells. *J Periodontal Res* 2011; 46: 427-437.

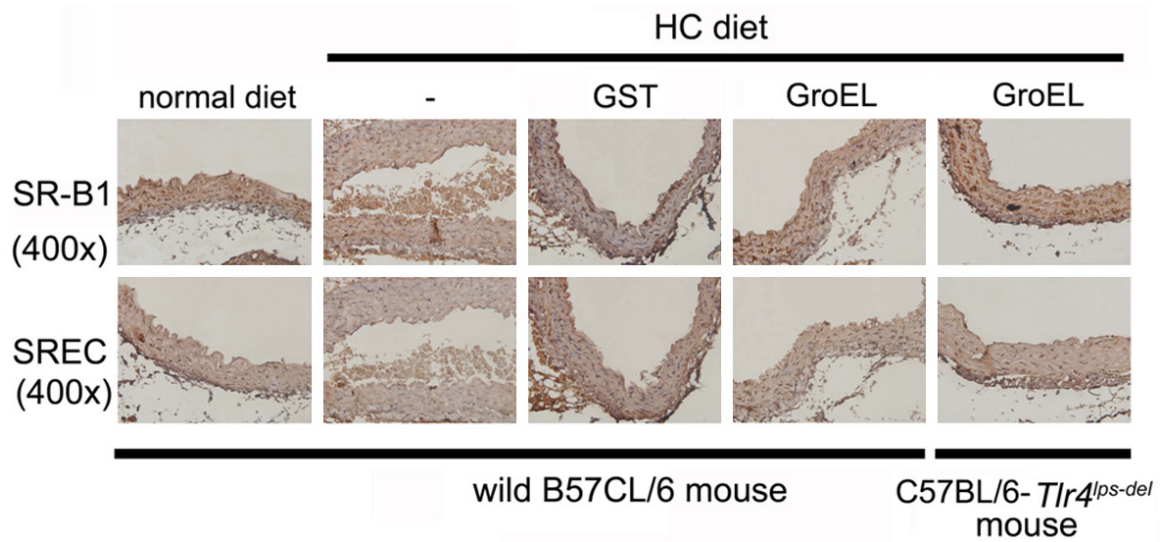
Porphyromonas gingivalis regulates atherogenesis

- [40] Champaiboon C, Poolgesorn M, Wisitrasameewong W, Sa-Ard-lam N, Rerkyen P and Mahanonda R. Differential inflammasome activation by *Porphyromonas gingivalis* and cholesterol crystals in human macrophages and coronary artery endothelial cells. *Atherosclerosis* 2014; 235: 38-44.
- [41] Huck O, Elkaim R, Davideau JL and Tenenbaum H. *Porphyromonas gingivalis* and its lipopolysaccharide differentially regulate the expression of cathepsin B in endothelial cells. *Mol Oral Microbiol* 2012; 27: 137-148.
- [42] Liu B, Cheng L, Liu D, Wang J, Zhang X, Shu R and Liang J. Role of p38 mitogen-activated protein kinase pathway in *Porphyromonas gingivalis* lipopolysaccharide-induced VCAM-1 expression in human aortic endothelial cells. *J Periodontol* 2012; 83: 955-962.
- [43] Turunen SP, Kummu O, Harila K, Veneskoski M, Soliymani R, Baumann M, Pussinen PJ and Horkko S. Recognition of *Porphyromonas gingivalis* gingipain epitopes by natural IgM binding to malondialdehyde modified low-density lipoprotein. *PLoS One* 2012; 7: e34910.
- [44] Lin FY, Huang CY, Lu HY, Shih CM, Tsao NW, Shyue SK, Lin CY, Chang YJ, Tsai CS, Lin YW and Lin SJ. The GroEL protein of *Porphyromonas gingivalis* accelerates tumor growth by enhancing endothelial progenitor cell function and neovascularization. *Mol Oral Microbiol* 2015; 30: 198-216.
- [45] Falck-Hansen M, Kassiteridi C and Monaco C. Toll-like receptors in atherosclerosis. *Int J Mol Sci* 2013; 14: 14008-14023.
- [46] Pollreis A, Huang Y, Roth GA, Cheng B, Kobschull M, Papapanou PN, Schmidt AM and Lalla E. Enhanced monocyte migration and pro-inflammatory cytokine production by *Porphyromonas gingivalis* infection. *J Periodontal Res* 2010; 45: 239-245.
- [47] Ao M, Miyauchi M, Inubushi T, Kitagawa M, Furusho H, Ando T, Ayuningtyas NF, Nagasaki A, Ishihara K, Tahara H, Kozai K and Takata T. Infection with *Porphyromonas gingivalis* exacerbates endothelial injury in obese mice. *PLoS One* 2014; 9: e110519.
- [48] Hokamura K, Inaba H, Nakano K, Nomura R, Yoshioka H, Taniguchi K, Ooshima T, Wada K, Amano A and Umemura K. Molecular analysis of aortic intimal hyperplasia caused by *Porphyromonas gingivalis* infection in mice with endothelial damage. *J Periodontal Res* 2010; 45: 337-344.
- [49] Sun W, Wu J, Lin L, Huang Y, Chen Q and Ji Y. *Porphyromonas gingivalis* stimulates the release of nitric oxide by inducing expression of inducible nitric oxide synthases and inhibiting endothelial nitric oxide synthases. *J Periodontal Res* 2010; 45: 381-388.
- [50] Hashizume T, Kurita-Ochiai T and Yamamoto M. *Porphyromonas gingivalis* stimulates monocyte adhesion to human umbilical vein endothelial cells. *FEMS Immunol Med Microbiol* 2011; 62: 57-65.
- [51] Pollreis A, Hudson BI, Chang JS, Qu W, Cheng B, Papapanou PN, Schmidt AM and Lalla E. Receptor for advanced glycation endproducts mediates pro-atherogenic responses to periodontal infection in vascular endothelial cells. *Atherosclerosis* 2010; 212: 451-456.
- [52] Fan MH, Wong KL, Wu S, Leung WK, Yam WC and Wong TM. Preconditioning with *Porphyromonas gingivalis* lipopolysaccharide may confer cardioprotection and improve recovery of the electrically induced intracellular calcium transient during ischemia and reperfusion. *J Periodontal Res* 2010; 45: 100-108.
- [53] Hayashi C, Papadopoulos G, Gudino CV, Weinberg EO, Barth KR, Madrigal AG, Chen Y, Ning H, LaValley M, Gibson FC 3rd, Hamilton JA and Genco CA. Protective role for TLR4 signaling in atherosclerosis progression as revealed by infection with a common oral pathogen. *J Immunol* 2012; 189: 3681-3688.
- [54] Maekawa T, Takahashi N, Tabeta K, Aoki Y, Miyashita H, Miyauchi S, Miyazawa H, Nakajima T and Yamazaki K. Chronic oral infection with *Porphyromonas gingivalis* accelerates atheroma formation by shifting the lipid profile. *PLoS One* 2011; 6: e20240.
- [55] Velsko IM, Chukkappalli SS, Rivera MF, Lee JY, Chen H, Zheng D, Bhattacharyya I, Gangula PR, Lucas AR and Kesavalu L. Active invasion of oral and aortic tissues by *Porphyromonas gingivalis* in mice causally links periodontitis and atherosclerosis. *PLoS One* 2014; 9: e97811.
- [56] Shaik-Dasthagirisahab YB, Huang N, Baer MT and Gibson FC 3rd. Role of MyD88-dependent and MyD88-independent signaling in *Porphyromonas gingivalis*-elicited macrophage foam cell formation. *Mol Oral Microbiol* 2013; 28: 28-39.
- [57] Michaud DS, Joshipura K, Giovannucci E and Fuchs CS. A prospective study of periodontal disease and pancreatic cancer in US male health professionals. *J Natl Cancer Inst* 2007; 99: 171-175.
- [58] Hujoel PP, Drangsholt M, Spiekerman C and Weiss NS. An exploration of the periodontitis-cancer association. *Ann Epidemiol* 2003; 13: 312-316.
- [59] Solomon MP, Biernacki J, Slippen M and Rosen Y. Parosteal osteogenic sarcoma of the mandible, Existence masked by diffuse periodontal inflammation. *Arch Otolaryngol* 1975; 101: 754-760.
- [60] Abnet CC, Kamangar F, Dawsey SM, Stolzenberg-Solomon RZ, Albanes D, Pietinen

Porphyromonas gingivalis regulates atherogenesis

- P, Virtamo J and Taylor PR. Tooth loss is associated with increased risk of gastric non-cardia adenocarcinoma in a cohort of Finnish smokers. *Scand J Gastroenterol* 2005; 40: 681-687.
- [61] Fitzpatrick SG and Katz J. The association between periodontal disease and cancer: a review of the literature. *J Dent* 2010; 38: 83-95.
- [62] Hagiwara M, Kurita-Ochiai T, Kobayashi R, Hashizume-Takizawa T, Yamazaki K and Yamamoto M. Sublingual vaccine with GroEL attenuates atherosclerosis. *J Dent Res* 2014; 93: 382-387.
- [63] Jeong E, Kim K, Kim JH, Cha GS, Kim SJ, Kang HS and Choi J. *Porphyromonas gingivalis* HSP60 peptides have distinct roles in the development of atherosclerosis. *Mol Immunol* 2015; 63: 489-496.
- [64] Bakheet T, Frevel M, Williams BR, Greer W and Khabar KS. ARED: human AU-rich element-containing mRNA database reveals an unexpectedly diverse functional repertoire of encoded proteins. *Nucleic Acids Res* 2001; 29: 246-254.
- [65] Lin FY, Tsai YT, Lee CY, Lin CY, Lin YW, Li CY, Shih CM, Huang CY, Chang NC, Tsai JC, Chen TL and Tsai CS. TNF-alpha-decreased thrombomodulin expression in monocytes is inhibited by propofol through regulation of tristetraprolin and human antigen R activities. *Shock* 2011; 36: 279-288.
- [66] Dean JL, Wait R, Mahtani KR, Sully G, Clark AR and Saklatvala J. The 3' untranslated region of tumor necrosis factor alpha mRNA is a target of the mRNA-stabilizing factor HuR. *Mol Cell Biol* 2001; 21: 721-730.
- [67] Peng SS, Chen CY, Xu N and Shyu AB. RNA stabilization by the AU-rich element binding protein, HuR, an ELAV protein. *EMBO J* 1998; 17: 3461-3470.
- [68] Lasa M, Mahtani KR, Finch A, Brewer G, Saklatvala J and Clark AR. Regulation of cyclooxygenase 2 mRNA stability by the mitogen-activated protein kinase p38 signaling cascade. *Mol Cell Biol* 2000; 20: 4265-4274.
- [69] Wang W, Caldwell MC, Lin S, Furneaux H and Gorospe M. HuR regulates cyclin A and cyclin B1 mRNA stability during cell proliferation. *Embo J* 2000; 19: 2340-2350.
- [70] Wang W, Furneaux H, Cheng H, Caldwell MC, Hutter D, Liu Y, Holbrook N and Gorospe M. HuR regulates p21 mRNA stabilization by UV light. *Mol Cell Biol* 2000; 20: 760-769.
- [71] Ming XF, Stoecklin G, Lu M, Looser R and Moroni C. Parallel and independent regulation of interleukin-3 mRNA turnover by phosphatidylinositol 3-kinase and p38 mitogen-activated protein kinase. *Mol Cell Biol* 2001; 21: 5778-5789.
- [72] Tsai CS, Chen DL, Lin SJ, Tsai JC, Lin TC, Lin CY, Chen YH, Huang GS, Tsai HY, Lin FY and Li CY. TNF-alpha inhibits toll-like receptor 4 expression on monocytic cells via tristetraprolin during cardiopulmonary bypass. *Shock* 2009; 32: 40-48.
- [73] Lai WS, Carballo E, Strum JR, Kennington EA, Phillips RS and Blackshear PJ. Evidence that tristetraprolin binds to AU-rich elements and promotes the deadenylation and destabilization of tumor necrosis factor alpha mRNA. *Mol Cell Biol* 1999; 19: 4311-4323.
- [74] Carballo E, Lai WS and Blackshear PJ. Evidence that tristetraprolin is a physiological regulator of granulocyte-macrophage colony-stimulating factor messenger RNA deadenylation and stability. *Blood* 2000; 95: 1891-1899.
- [75] Stoecklin G, Ming XF, Looser R and Moroni C. Somatic mRNA turnover mutants implicate tristetraprolin in the interleukin-3 mRNA degradation pathway. *Mol Cell Biol* 2000; 20: 3753-3763.
- [76] Carballo E, Lai WS and Blackshear PJ. Feedback inhibition of macrophage tumor necrosis factor-alpha production by tristetraprolin. *Science* 1998; 281: 1001-1005.

Porphyromonas gingivalis regulates atherogenesis



Supplementary Figure 1. There were no atherosclerotic lesions in the aortas of any group. The graphs show 400x magnification of the slide. Immunohistochemistry to assess SR-B1 and SREC in mouse aortas. The lumen is uppermost in all sections, and corresponding hematoxylin staining was used to identify the nucleus.